



Titre: Experimental Study of Volumetric Gas-Liquid Mass Transfer
Title: Coefficient in Slurry Bubble Columns

Auteur: Afshin Fallahi
Author:

Date: 2019

Type: Mémoire ou thèse / Dissertation or Thesis

Référence: Fallahi, A. (2019). Experimental Study of Volumetric Gas-Liquid Mass Transfer
Citation: Coefficient in Slurry Bubble Columns [Mémoire de maîtrise, Polytechnique
Montréal]. PolyPublie. <https://publications.polymtl.ca/3874/>

 **Document en libre accès dans PolyPublie**
Open Access document in PolyPublie

URL de PolyPublie: <https://publications.polymtl.ca/3874/>
PolyPublie URL:

**Directeurs de
recherche:** Jamal Chaouki
Advisors:

Programme: Génie chimique
Program:

POLYTECHNIQUE MONTRÉAL

affiliée à l'Université de Montréal

**Experimental study of volumetric gas-liquid mass transfer coefficient in slurry
bubble columns**

AFSHIN FALLAHI

Département de génie chimique

Mémoire présenté en vue de l'obtention du diplôme de *maîtrise ès sciences appliquées*

Génie chimique

Mai 2019

© Afshin Fallahi, 2019.

POLYTECHNIQUE MONTRÉAL

affiliée à l'Université de Montréal

Ce mémoire intitulé :

Experimental study of volumetric gas-liquid mass transfer coefficient in slurry bubble columns

présenté par **Afshin FALLAHI**

en vue de l'obtention du diplôme de *Maîtrise ès sciences appliquées*

a été dûment accepté par le jury d'examen constitué de :

Abdellah AJJI, président

Jamal CHAOUKI, membre et directeur de recherche

Mohammad LATIFI, membre

ACKNOWLEDGEMENTS

I would like to express my sincere gratitude to Professor Jamal Chaouki for his valuable guidance and support throughout this study. He provided me the opportunity to work on this challenging project and always gave me intellectual freedom.

I am deeply grateful to El Mahdi Lakhdissi for his guidance and help with the experimental part of my research. I benefited from our discussions and his invaluable comments and suggestions on my thesis. I would also like to thank him for the translation of the abstract to French.

I would like to thank my dear friend and colleague, Mojtaba Mokhtari, for his valuable contribution and help, and constructive comments on my thesis.

Many thanks to my colleagues at PEARL research group, from whom I learned a great deal during our meetings and friendly discussions.

The technical support of the department of Chemical Engineering, particularly Mr. Robert Delisle and Mr. Sylvain Simard-Fleury is greatly appreciated.

I acknowledge the financial support provided by Total E&P and Natural Sciences and Engineering Research Council of Canada (NSERC).

I dedicate this work to my wife, Maryam, and my son, Mahyar.

Afshin Fallahi

RÉSUMÉ

Les colonnes à bulles slurry (SBCRs) sont largement utilisées dans une multitude de procédés où le contact efficace entre les phases gazeuse, liquide et solide est d'une importance critique. Dans ce contexte, les SBCRs ont trouvé beaucoup d'applications lors de la dernière décennie dans plusieurs industries chimiques, biochimiques et pétrochimiques. Les colonnes à bulles offrent plusieurs avantages à savoir un transfert de chaleur et de masse élevé, des coûts d'opération et de maintenance diminués, un excellent mélangeage des différentes phases, une distribution uniforme de la température et aussi de la compacité. Il est déjà établi qu'une compréhension complète des phénomènes de transfert de matière est essentielle pour le design et la mise en échelle des SBCRs. Or, ces deux tâches s'avèrent difficiles à réaliser du fait que la vitesse de transfert de matière est liée directement aux dimensions du réacteur, aux conditions opératoires et aux propriétés physiques de chacune des phases. Malgré le nombre d'études qui ont été menées sur l'effet des particules solides sur l'hydrodynamique et le transfert de matière dans les colonnes à bulles, il n'y a pas encore un accord sur le mécanisme dominant et aussi sur son amplitude. Plus important, la majorité des travaux antérieurs ont été réalisées dans des réacteurs à échelle laboratoire pour étudier l'effet des particules solides. Par conséquent, les résultats peuvent s'avérer non pertinent du fait que l'hydrodynamique change quand on passe de l'échelle laboratoire à l'échelle industrielle.

Pour aborder cette problématique, une colonne à bulles slurry à échelle pilote a été utilisée dans ce travail pour étudier le coefficient volumétrique de transfert de matière gaz-liquide ($k_L a$) dans un système biphasique (air-eau) et triphasique (air-eau-billes de verre). L'effet de la vitesse superficielle du gaz, la concentration et la taille des particules sur le $k_L a$ a été étudié expérimentalement. Les résultats obtenus ont été justifiés en considérant l'hydrodynamique et les différentes théories de transfert de matière applicables aux colonnes à bulles. Dans la dernière partie de cette étude, une corrélation fiable a été développée pour estimer le coefficient de transfert de matière en se basant sur les conditions opératoires, les grandeurs du design et les propriétés des trois phases.

Pour l'effet de la vitesse superficielle du gaz dans le système air-eau, nous avons observé que l'augmentation de la vitesse du gaz (entre 0.4 et 21.3 cm/s) augmente le coefficient de transfert de matière. Ceci peut être attribué à un meilleur mélangeage entre les phases liquide et gazeuse et

aussi à la rétention de gaz élevée. Aussi, un résultat intéressant est que, indépendamment de la vitesse de gaz, la variation du coefficient de transfert de matière dans la direction radiale est négligeable ce qui peut être attribué à la rapidité du mélangeage de la phase liquide dans la colonne. Nous avons aussi observé que la concentration (0, 1, 3, and 5% v/v) et la taille (71 and 156 μm) des particules solides (i.e. Billes de verre) affectent fortement la vitesse de transfert de matière. L'effet de la phase solide sur le $k_L a$ est dépendant de la vitesse du gaz. Pour les faibles vitesses, la présence des particules solides a un effet négatif sur le transfert de matière tandis qu'à hautes vitesses, le solide fait augmenter le transfert de matière. Les billes de verre à diamètre élevé (i.e. 156 μm) ont fait augmenter le coefficient de transfert de matière de manière notable et ceci est dû principalement à l'augmentation de la turbulence dans l'interface gaz-liquide à cause de la présence des particules. La corrélation développée pour estimer le coefficient de transfert de matière dans les systèmes biphasiques et triphasiques comprend Schmidt, Galilei, Froude, Bond, la densité du gaz et du liquide, la diffusivité de l'oxygène et le diamètre de la colonne. La corrélation développée a pu reproduire les résultats expérimentaux avec succès : Erreur absolue moyenne < 4.81% et écart type ~ 0.27 %.

ABSTRACT

Slurry bubble column reactors (SBCRs) are extensively employed in a variety of processes in which efficient contact between the gas, liquid, and solid phases are of critical importance. In this context, in the past decade, SBCRs have found numerous applications in chemical, biochemical, and petrochemical industries. Bubble column reactors offer a number of advantages: superior heat and mass transfer rates, low operating and maintenance costs, excellent mixing of solids, uniform temperature distribution, and compactness. It is well established that a comprehensive understanding of the mass transfer phenomena is essential in order to design and scale-up SBCRs for industrial purposes. The fact that the mass transfer rate is connected to a large number of factors including reactor dimensions, operating conditions, physical properties of each phase makes the problem even more complicated. Despite the fact that there are several studies on the impact of solid particles on hydrodynamics and mass transport in SBCRs, still, there is no general agreement regarding the prevailing mechanism or the magnitude of such effect. More importantly, the majority of previous studies utilized laboratory scale test rig to investigate the role of solid particles; thus, the results may not be relevant to large scale reactors mainly due to the differences in hydrodynamics.

To address these research gaps, in the present study, a pilot scale slurry bubble column has been used to investigate the volumetric gas-liquid mass transfer coefficient ($k_L a$) in two-phase (air-water) and three-phase (air-water-glass beads) systems. The influence of superficial gas velocity, solid particle concentration, and solid particle size on $k_L a$ were experimentally explored. The obtained results were justified by taking into account the hydrodynamics, various mass transfer theories applicable to SBCRs. In the last part of the study, a reliable model (i.e. correlation) was developed to estimate the mass transfer coefficient based on the operating conditions, design variables and the properties of the three phases.

Regarding the effect of superficial gas velocity in the air-water system, it was observed that increasing the gas velocity (in a wide range of 0.40-21.30 cm/s) leads to a higher mass transfer rate. This can be attributed to the better contact between the liquid and gas phase, and the more gas holdup. Interestingly, it was noted that regardless of the gas velocity, the variation in the mass transfer coefficient in the radial direction is not significant, which can be partly ascribed to the high

liquid phase mixing in the column. It was found that the concentration (0, 1, 3, and 5% v/v) and size (71 and 156 μm) of solid particles (i.e. glass beads) strongly affect the behavior of the system and the mass transfer rate. The effect of the solid phase on $k_L a$ depends on the gas velocity. In low gas velocities, the presence of solid particles adversely affects the mass transfer, while at high velocities, solids particles are beneficial. Using large size glass beads (i.e. 156 μm) caused a noticeable improvement in the mass transfer coefficient, mainly due to turbulence increasing in the gas-liquid interface by the particles. The developed correlation for predicting the mass transfer coefficient in two and three-phase systems incorporates Schmidt, Galilei, Froude and Bond numbers, and gas and liquid density, oxygen diffusivity, and column diameter. The developed correlation could reproduce the experimental data successfully: mean absolute percentage error $< 4.81\%$ and standard deviation $\sim 0.27\%$.

TABLE OF CONTENTS

| | |
|---|------|
| ACKNOWLEDGEMENTS | III |
| RÉSUMÉ..... | IV |
| ABSTRACT | VI |
| TABLE OF CONTENTS | VIII |
| LIST OF TABLES | X |
| LIST OF FIGURES..... | XI |
| LIST OF SYMBOLS AND ABBREVIATIONS..... | XI |
| CHAPTER 1 INTRODUCTION..... | 1 |
| 1.1 Problem Statement and Motivation..... | 1 |
| 1.2 Objectives..... | 3 |
| CHAPTER 2 LITERATURE REVIEW..... | 4 |
| 2.1 Slurry bubble columns | 4 |
| 2.1.1 Concept, types, and applications | 4 |
| 2.1.2 Design and operation..... | 6 |
| 2.1.3 Hydrodynamics | 7 |
| 2.1.4 Dynamics of gas bubbles..... | 16 |
| 2.2 Mass transfer | 17 |
| 2.2.1 Theories | 17 |
| 2.2.2 Volumetric mass transfer coefficient, kLa | 21 |
| 2.2.3 Mass transfer measurement techniques | 25 |
| CHAPTER 3 EXPERIMENTAL AND METHODOLOGY | 27 |
| 3.1 Materials..... | 27 |
| 3.2 Experimental Setup | 28 |

| | | |
|--|---|----|
| 3.3 | Measurement of volumetric mass transfer coefficient | 30 |
| CHAPTER 4 RESULTS AND DISCUSSION | | 31 |
| 4.1 | Effect of superficial gas velocity | 31 |
| 4.2 | Radial distribution of volumetric mass transfer coefficient | 34 |
| 4.3 | Effect of solid concentration | 36 |
| 4.4 | Effect of particle size | 41 |
| 4.5 | Developing a new model for predicting <i>kLa</i> | 42 |
| 4.5.1 | Dimensionless analysis to derive correlation | 42 |
| 4.5.2 | Applying developed correlation to previous experimental results | 46 |
| 4.5.3 | Comparison of the present correlation with other correlations | 48 |
| CHAPTER 5 CONCLUSION AND RECOMMENDATIONS | | 50 |
| 5.1 | Conclusion | 50 |
| 5.2 | Recommendations | 51 |
| REFERENCES | | 52 |

LIST OF TABLES

| | |
|--|----|
| Table 2.1- Experimental study of the transition regime in the bubble columns (Air-Water) [7, 36] | 10 |
| Table 2.2- Correlations for predicting (α) and (kL) in BCs and SBCs | 22 |
| Table 3.1- Physical properties of materials in this work..... | 27 |
| Table 3.2- Operating conditions and geometrical specifications of the BC with distributor..... | 28 |
| Table 4.1- Solubility of oxygen in water at various temperatures and atmospheric pressure. (MAPE = 1.3 %) | 33 |
| Table 4.2- Dimensionless numbers used in this work..... | 43 |
| Table 4.3- Formulas for calculating density, viscosity, and diffusivity of the slurry phase | 44 |
| Table 4.4- Literature list for the SBCs parametric study | 47 |
| Table 4.5- Dimensionless correlations for prediction of kLa in BCs in some literature | 48 |

LIST OF FIGURES

| | |
|--|----|
| Figure 2.1- Sketch of different types of bubble column reactors. Adapted from reference [24] | 5 |
| Figure 2.2- Variables and phenomena affecting the performance of bubble columns. Adapted from reference [25] | 6 |
| Figure 2.3- Schematic of the flow regimes in bubble column reactors. Adapted from reference [24] | 7 |
| Figure 2.4- Flow regime diagram in bubble columns depending on gas velocity and column diameter. Adapted from reference [24] | 9 |
| Figure 2.5- Parameters influencing the Performance of the Slurry Bubble Column Reactor. Adapted from reference [33] | 12 |
| Figure 2.6- Gas holdup variation with superficial gas velocity. Adapted from reference [44] | 13 |
| Figure 2.7- Schematic of two film theory. “Mass transfer results from molecular diffusion via the film”. Adapted from reference [83]..... | 18 |
| Figure 2.8- Schematic of Higbie’s model. “Each liquid element is in contact with the gas phase for the same amount of time”. Adapted from reference [5]..... | 19 |
| Figure 2.9- Schematic of Surface-renewal theory. “Liquid elements at the interface are randomly changed by fresh elements from the bulk”. Adapted from reference [4] | 20 |
| Figure 2.10- Sketch of oxygen transfer from the air bubble into the water based on two film theory. Adapted from reference [83] | 24 |
| Figure 3.1- (a) Schematic of experimental set-up (b) Photograph of optical dissolved oxygen probe (VisiPerm DO325, Hamilton Inc.) | 29 |
| Figure 4.1- Dissolved oxygen concentration variation for air–water system. | 31 |
| Figure 4.2- Radial distribution of volumetric mass transfer coefficient in the air-water system... | 34 |
| Figure 4.3- Radial distribution of kLa in the air-water system..... | 35 |
| Figure 4.4- Impact of UG on the kLa - (a) Air-Water-Glass beads $71\mu m$ - (b) Air-Water-Glass beads $156\mu m$ | 37 |

| | |
|--|----|
| Figure 4.5- Impact of solid particles concentration on the kLa at different UG -(a) Air-Water-Glass beads $71\mu m$, (b) Air-Water-Glass beads $156\mu m$ | 39 |
| Figure 4.6- Effect of particle size on kLa at a constant solid concentration..... | 41 |
| Figure 4.7- Comparison between the experimental and the predicted value of kLa | 45 |
| Figure 4.8- Applying developed a correlation of kLa to previous experimental works | 46 |
| Figure 4.9- Comparison between some proposed correlations for predicting kLa | 49 |

LIST OF SYMBOLS AND ABBREVIATIONS

Nomenclature

| | |
|-------------|--|
| a | Interfacial area [$1/m$] |
| C_0 | The dissolved oxygen concentration in the water ($t = 0$) [mg/L] |
| C_i | The dissolved oxygen concentration in the gas – liquid interface [mg/L] |
| C_{DO} | The dissolved oxygen concentration in the water (C_L) [mg/L] |
| $C_{O_2}^*$ | The dissolved oxygen concentration in the water in equilibrium with P_{O_2} [mg/L] |
| C_V | Volumetric solid concentration |
| d_0 | Orifice diameter [mm] |
| d_b | Spherical bubble diameter [m] |
| d_{BPPS} | Bubble Plate (gas distributor)Pore Size (in the reference [1]) [m] |
| d_p | Solid particle mean diameter [μm] |
| d_s | Sauter mean bubble diameter in the reference [2] [m] |
| d_{vs} | volume – surface mean bubble diameter (in the reference [3]) [m] |
| D_C | Column diameter [m] |
| D_G | Molecular diffusivity of oxygen from the water to the air bubbles [m^2/s] |
| D_L | Molecular diffusivity of oxygen from the air bubbles to the water [m^2/s] |
| g | Gravitational constant [m/s^2] |
| H | Henry constant [$mol/m^3 \cdot atm$] |
| H_0 | Initial liquid height [m] |
| H_C | Column height [m] |
| J_{O_2} | The molar flux of oxygen from the air bubble through the water [$mol/m^2 \cdot s$] |
| j_{GL} | Drift flux velocity [m/s] |

| | |
|-------------|---|
| k_G | Local gas – phase mass transfer coefficient [m/s] |
| K_G | Overall gas – phase mass transfer coefficient [m/s] |
| k_L | Local liquid – phase mass transfer coefficient [m/s] |
| K_L | Overall liquid – phase mass transfer coefficient [m/s] |
| $k_L a$ | Volumetric liquid phase mass transfer coefficient [$1/s$] |
| N_{O_2} | Oxygen mass transfer rate per unit volume [$mol/m^2.s$] |
| P_i | Oxygen partial pressure in the gas – liquid interface [atm] |
| P_{O_2} | Oxygen partial pressure in the air bubble bulk [atm] |
| $P_{O_2}^*$ | Oxygen partial pressure in equilibrium with liquid phase [atm] |
| s | Surface renewal rate related to the rate of production of the fresh surface [4] |
| t | Time variable [s] |
| T | Temperature [$^{\circ}C$] |
| U_G | Superficial gas velocity [m/s] |
| U_L | Superficial liquid velocity [m/s] |
| V_G | Gas volume in SBC [m^3] |
| V_L | Liquid volume in SBC [m^3] |
| V_S | Solid volume in SBC [m^3] |
| V_T | The total volume of the three – phase in slurry bubble column [m^3] |

Dimensionless numbers

| | |
|------|--|
| Bo | Bond number = $g\rho_L D_C^2 / \sigma_L$ |
| Fr | Froude number = $U_G / \sqrt{gd_B}$ |
| Ga | Galilei number = $g\rho_L^2 D_C^3 / \mu_L^2$ |
| Sc | Schmidt numbr = $\mu_L / \rho_L D_L$ |

Greek letters

| | |
|-----------------|--|
| δ_G | The film thickness in the gas phase [m] |
| δ_L | The film thickness in the liquid phase [m] |
| ε_G | Gas holdup [–] |
| ε_i | The holdup of phase i [–] |
| μ_L | Liquid viscosity [kg/m.s] |
| μ_{SL} | Slurry viscosity [kg/m.s] |
| ρ_G | Gas density [kg/m ³] |
| ρ_L | Liquid density [kg/m ³] |
| ρ_S | Solid density [kg/m ³] |
| ρ_{SL} | Slurry density [kg/m ³] |
| σ_L | Surface tension [N/m] |
| ϕ_L | The volume fraction of the liquid phase [–] |
| ϕ_S | The volume fraction of the solid phase [–] |
| θ | Contact time according to penetration theory [5] |

Abbreviations

| | |
|------|---|
| BC | Bubble column |
| BCR | Two-Phase bubble column reactor |
| DO | Dissolved Oxygen concentration |
| MAPE | Mean absolute percentage error |
| SBC | Slurry bubble column |
| SBCR | Liquid- Solid suspension (Slurry bubble column reactor) |
| SD | Standard deviation |

CHAPTER 1 INTRODUCTION

1.1 Problem Statement and Motivation

Bubble column reactors have been used extensively in the past 40 years as gas-solid-liquid contactors and reactors in numerous chemical processes including gas-liquid Fischer-Tropsch synthesis [6], coal liquefaction, hydrodesulphurization, hydrogenation, and biological wastewater treatment [7]. In comparison to other multi-phase reactors, BCR offers far better heat and mass transfer rates, easy maintenance, low capital cost and the possibility of using fine solid catalysts and adding fresh catalysts without shutting down the entire system. Mass transfer rates between different phases significantly influence the performance of BCR and are of great importance in the design and scale-up of this technology [8]. Despite the wealth of research in this area, still, there are many unanswered questions regarding the mass transfer mechanisms in BCR due to the complexity of the system once other influencing factors including fluid dynamics, the chemistry of solution, and solid particle properties are to be taken into account. The main factors that can affect the mass transfer rate in BCR are (i) properties of each phase (ii) operating conditions (including temperature, pressure, and gas velocity), and (iii) reactor dimensions and internals design [9]. In fact, these parameters can affect the gas-liquid mass transfer coefficient and the specific interfacial area between the gas and liquid phase. The influence of the various parameters on the mass transfer coefficient and the interfacial area is discussed in chapter 2.

The liquid side mass transfer coefficient is often the limiting step in the overall mass transfer for many industrial situations in the bubble columns and the slurry bubble columns. The $k_L a$ decreases significantly in large scale reactors [10], and leads to complexity in the reactor design and scale-up. Many researchers investigated the effect of various parameters on $k_L a$ in slurry bubble columns [11-13]. However, the majority of them are done in a laboratory-scale [13] despite the need to know the $k_L a$ in the actual industrial condition in order to have a reliable large-scale design.

Besides, in most of the industrial applications of SBCRs, the solid particles use as a catalyst to increase the reaction rate and consequently decrease the reactor size. Obviously, the presence of solid particles in the liquid phase changes the apparent viscosity and density of the slurry phase. Therefore, hydrodynamic parameters of the system are changed and consequently, the mass transport rate is also changed. However, considering the complex interaction between so many

phenomena within slurry bubble column reactors, the exact mechanism through which solid phase alters the gas-liquid-solid processes is still a matter of debate. In addition, the impact of the solid concentration and solid physical properties on the overall mass transfer rate has not been fully investigated. Researchers reported various contradictory results about the effect of solid particles on $k_L a$. Some of them observed an increment in the volumetric mass transfer coefficient by adding the solid particle into the system [14]. In contrast, other researchers reported that the presence of the particles leads to a decrease in $k_L a$.

It should be mentioned that the measurement technique itself can be an important issue for measuring the $k_L a$. The measurement techniques can be divided into direct methods and indirect methods [15]. Direct methods include various methods such as mass spectrometry, dissolve oxygen probe and Polarographic Electrode. Indirect methods use the variations of a specific parameter (such as pressure drop and solution volume) in order to estimate the mass transfer coefficient. So, the direct methods are more accurate.

In the present study, investigations on the bubble column and slurry bubble column are done to define the effect of solid particles and the process conditions on $k_L a$. A pilot scale slurry bubble column has been utilized for the experimental investigations. Air, water and glass beads are used as materials and a dissolve oxygen probe, as a direct measurement technique, is utilized to measure the local oxygen concentration in the bubble column. The influence of superficial gas velocity (in various flow regimes), solid particle concentration, and particle size on $k_L a$ were experimentally explored. After that, a reliable correlation was proposed to estimate the volumetric mass transfer coefficient based on the operating conditions, design variables and the physical properties of the materials.

1.2 Objectives

Mass transfer rate is one of the most important parameters that should be determined in advance to precisely design bubble columns. From an economical point of view, increasing the mass transfer rate is highly wanted and is one of the basic problems in industries.

The overall objective of the present study is the experimental investigation of the volumetric mass transfer coefficient in a pilot-scale slurry bubble column reactor. To do so, the following sub-objectives were performed.

- ❖ Objective 1: Experimental study of the volumetric mass transfer coefficient in the bubble column to define the effect of process parameters on the radial $k_L a$.
- ❖ Objective 2: Define the effect of the particle size and concentration on the $k_L a$ in the slurry bubble column
- ❖ Objective 3: Develop a new correlation for predicting the volumetric gas-liquid mass transfer coefficient for slurry bubble columns

CHAPTER 2 LITERATURE REVIEW

2.1 Slurry bubble columns

2.1.1 Concept, types, and applications

Multiphase reactors are solid-liquid-gas contactors and reactors in which chemical reactions can take place [16]. Multiphase reactors are typically divided into three main categories, namely, trickle bed, fluidized bed, and bubble column reactors [7]. A bubble column reactor is basically a vertical column in which the gas phase in the form of bubbles are dispersed at the bottom of the column into a liquid phase (Two- phase bubble column (BCR)) or liquid- solid suspension (Slurry bubble column reactors (SBCR)) [7]. SBCRs have attracted tremendous attention in various industries and have been extensively employed in chemical and environmental processes [17-19]. In particular, BCRs are used in biotechnology, petrochemical processes, oxidation, hydrogenation of unsaturated oils, polymerization, alkylation and chlorination, effluent/wastewater treatment process, flotation and metallurgical operations (leaching of metal ores) [20], Fischer-Tropsch (FT) [21], catalytic chlorination of alkenes [18] and the hydro-conversion of petroleum residues and heavy oils [22]. Bubble column reactors offer a number of advantages in design and operation as compared to other reactors, which grant them enormous popularity and applicability in many fields. Bubble column reactors have unique mass and heat transfer characteristics which lead to high mass and heat coefficient due to enhanced dispersion of gas into liquid [20]. Additionally, simple design, low operating cost, and maintenance due to the lack of any mechanically operated parts, low energy input needed and high durability of catalysts are other positive aspects of BCRs [20]. On the other hand, the possibility of online catalyst addition and withdrawal ability and plug-free operation are other merits of these systems. The bubble column can be designed to work in either semi-batch mode (the superficial liquid velocity of $U_L \cong 0$) or in continuous mode (either co-currently ($U_L > 0$) or counter-currently ($U_L < 0$)) [23]. Figure 2-1 illustrates several types of bubble column reactors.

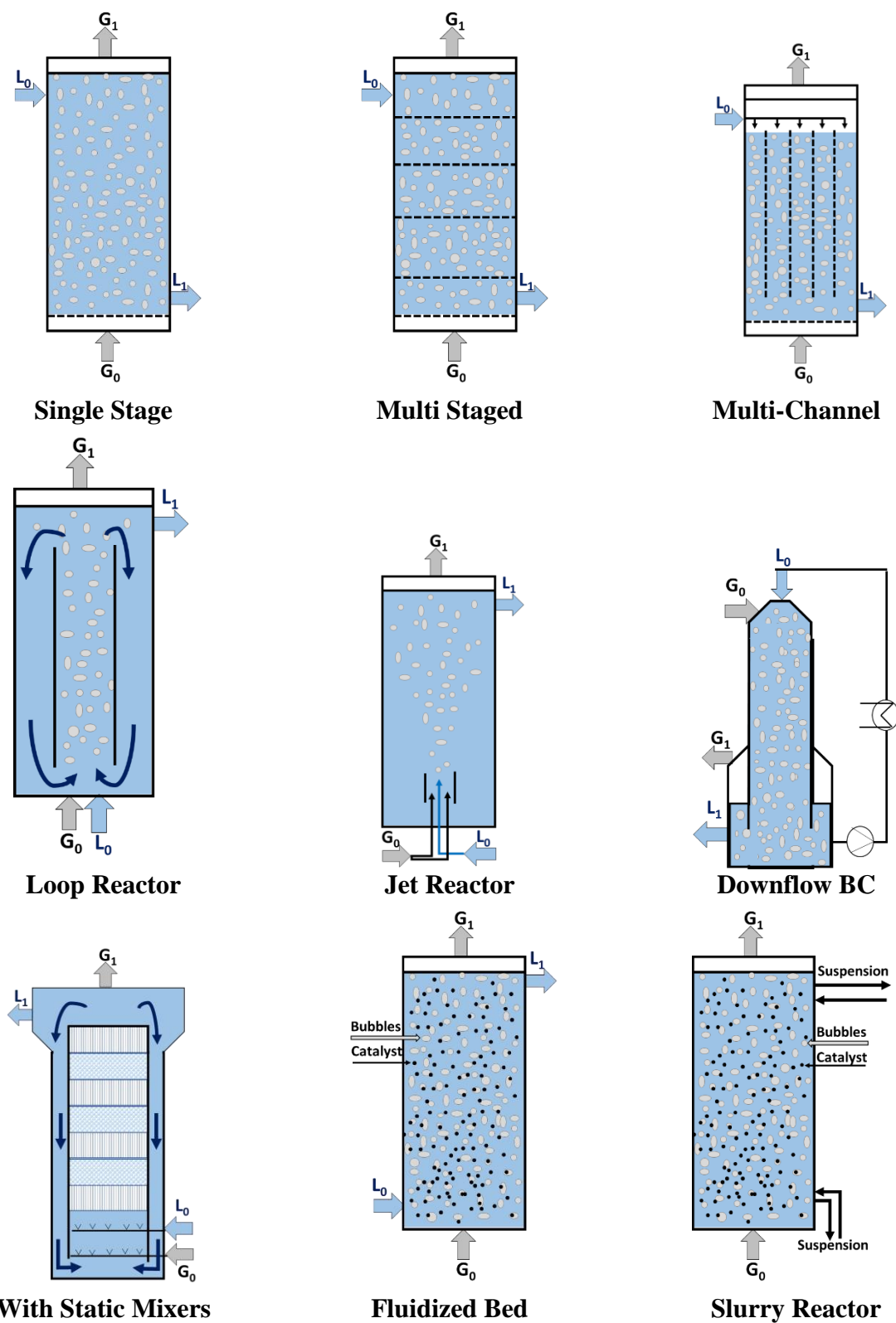


Figure 2.1- Sketch of different types of bubble column reactors. Adapted from reference [24]

2.1.2 Design and operation

During the design and scale-up of BCRs, three main phenomena should be taken into consideration: (i) heat and mass transfer characteristics; (ii) mixing characteristics; (iii) chemical kinetics of the reacting system. In line with this, the performance of a bubble column reactor strongly depends on a number of interconnected variables and processes. Figure 2-2 provides some of the key parameters and steps that determine the overall efficiency of bubble columns. Reaction orders with respect to reactants and products, rate constant, liquid- and solid- side mass transfer coefficients are extremely influential. In BCRs a stream of gas (dispersed phase) in the form of bubbles is injected into a liquid phase (continuous phase); accordingly, it is essential to understand the hydrodynamic aspects of the gas phase. Important parameters that influence hydrodynamics and mass transfer rate in SBCRs are flow regimes, gas holdup, bubble shape, bubble size, rise velocity, back mixing, pressure and temperature, the chemistry of gas/liquid/solid, solid particles properties, and reactor dimensions and design.

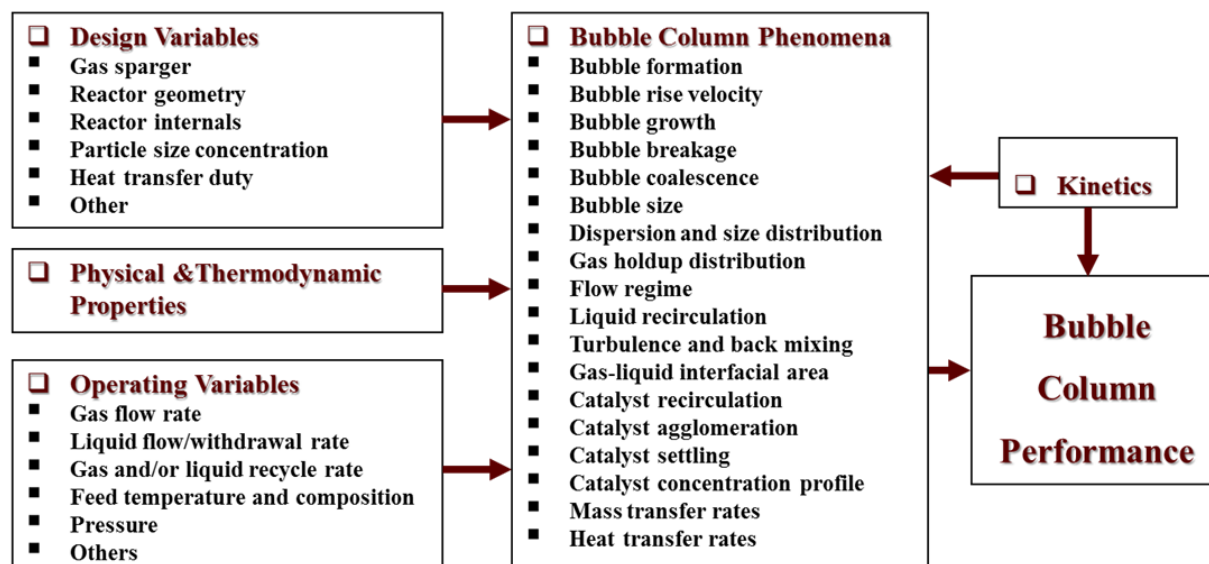


Figure 2.2- Variables and phenomena affecting the performance of bubble columns. Adapted from reference [25]

2.1.3 Hydrodynamics

It is widely acknowledged that the operating conditions, design, and geometry of the column impact the hydrodynamics of the SBCRs [26-28]. The key hydrodynamic parameters of bubble column reactors are discussed in the following sections.

2.1.3.1 Flow regime

The flow regimes in bubble column reactors are of three types: homogeneous flow regime (bubbly flow), heterogeneous flow regime (churn-turbulent), and slug flow regime, which are essentially defined by the operating conditions (mainly the superficial gas velocity) (depicted in Figure 2-3).

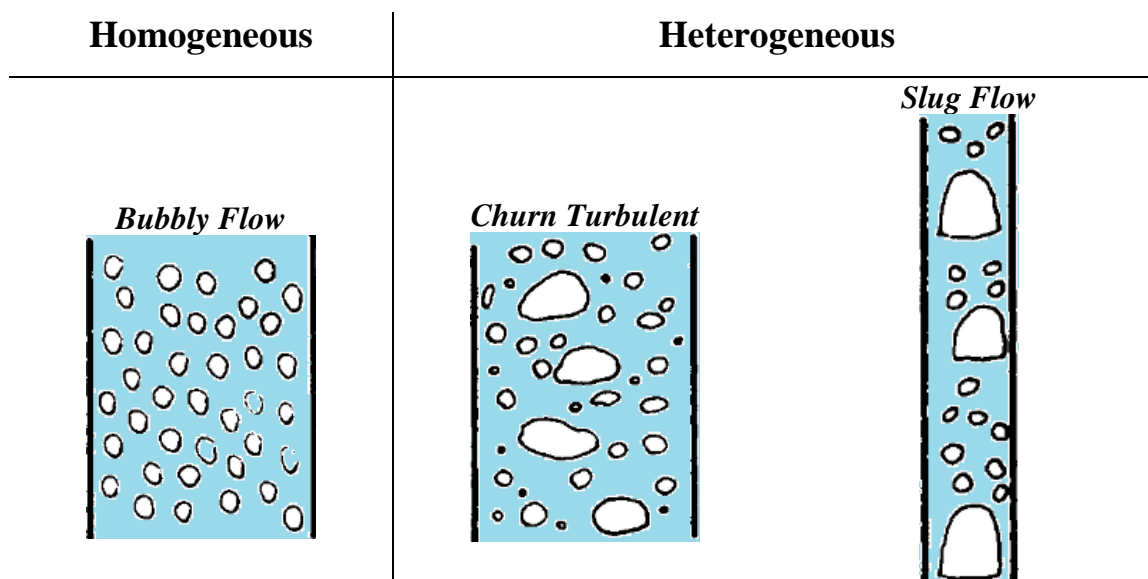


Figure 2.3- Schematic of the flow regimes in bubble column reactors. Adapted from [24]

The homogeneous flow regime (perfect or bad bubbly flow) is usually seen at low superficial gas velocities, (3-8 cm/s in semi-batch bubble columns) [29]. This flow regime is marked by a narrowed bubble size distribution and the generated bubbles are relatively spherical and have uniform small sizes (1–7 mm [30]).

A uniform bubble distribution and fairly mild mixing are witnessed over the entire cross-sectional area of the column [31]. There is no bubble coalescence or breakage in this regime, therefore, the

size of bubbles is controlled by gas sparger design and also properties of the system [32]. In this regime, the gas bubbles do not influence the motion of the liquid motion and almost no liquid mixing is observed [33].

The heterogeneous flow regime is marked by a wide bubble size distribution and generated bubbles are non-uniform in both small and large sizes. This type of regime is obtained at high superficial gas velocities (greater than 5 cm/s in batch columns) or when gas sparger generates large bubble via large size orifices [34]. In a heterogeneous flow regime, there is severe bubble coalescence and breakage, so, there are different sizes of bubbles in the column [7]. Due to the harsh turbulent motion of gas bubbles and liquid recirculation unsteady flow patterns and large bubbles with short residence times are formed by coalescence [7]. This flow regime is often seen in industrial-size and large diameter columns [31]. Despite the fact that the gas–liquid mass transfer coefficient is lower at heterogeneous regime (compared to homogeneous flow), BCRs are normally run under heterogeneous flow conditions in the chemical industry. Slug flow regime, characterized by bullet-shaped bubbles (extended over the entire column diameter), occurs in laboratory columns with small diameters and at high gas velocities [7]. This regime is formed as a result of the formation of bubble slugs when larger bubbles are stabilized by the column wall [29].

Between these two flow regimes (homogeneous and heterogeneous), there is a transition flow regime where the stability of the system from homogeneous flow regime decreases and a large circulation is forming due to a cluster of bubbles [34]. Figure 2-4 shows those regimes based on superficial gas velocity versus reactor diameter, where the shaded region indicates the transition flow regime [29]. This map is valid for both bubble and slurry bubble columns with a batch liquid phase operated with a low viscosity liquid phase. When the gas velocity is low (< 0.04 m/s), the BCR usually operates in the homogeneous flow regime and the column diameter has little impact on the flow regime. For columns with very small diameters, an increase in gas velocity can change the flow regime and formation of slugs will be observed.

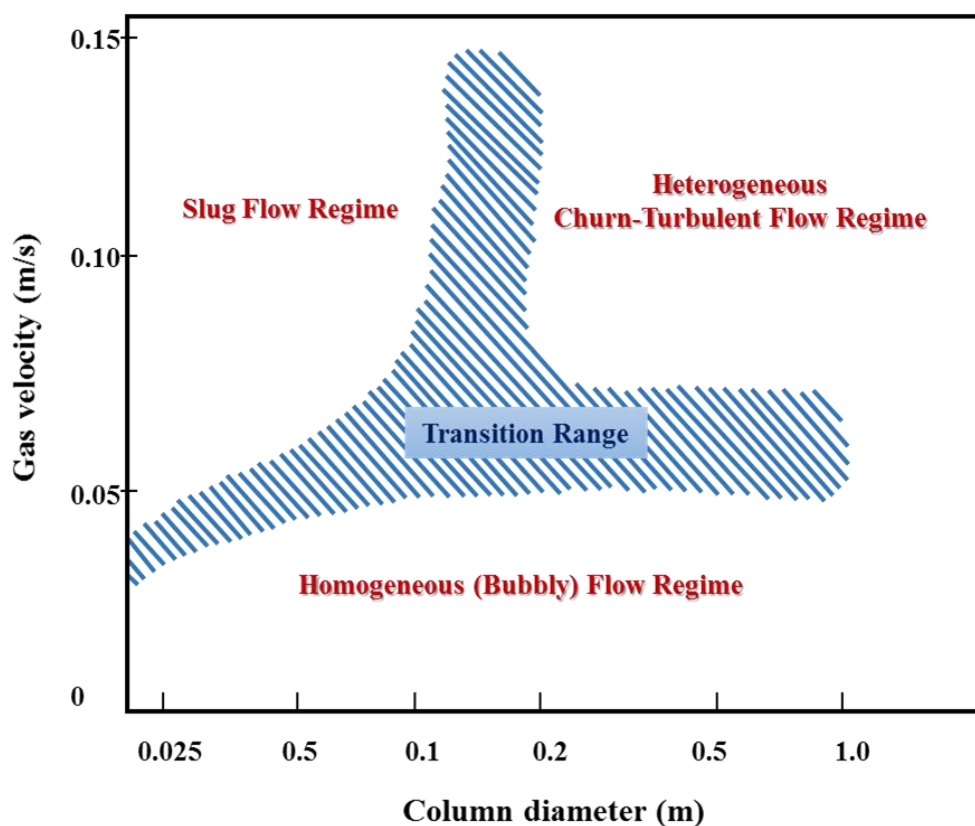


Figure 2.4- Flow regime diagram in bubble columns depending on gas velocity and column diameter. Adapted from reference [24]

Knowing the conditions at which regime transition from homogeneous to turbulent take place is quite important since significant changes are noted in the hydrodynamic behavior of the system. Thorat and Joshi [32] proposed that the transition gas velocity depends on the diameter and height of the column (aspect ratio (L/D)), sparger design, and physical properties of the system. Sarrafi et al. [35] conducted a comprehensive study on the existing literature on the transition superficial gas velocity and concluded that generally, the velocity falls in the range of 0.044-0.067 m/s. Table 2-1 lists the results of the literature studies with an air–water system for the regime transition properties.

Table 2.1- Experimental study of the transition regime in the bubble columns (Air-Water) [7, 36]

| Researcher(s) | Transition velocity (m/s) | Transition gas holdup (%) |
|-----------------------------------|----------------------------------|----------------------------------|
| Krishna et al. [37] | 0.0330 | 19.8 |
| Yamashida & Inoue [38] | 0.0400 | 23.4 |
| Hyndman et al. [31] | 0.0370 | 13.7 |
| Bach & Philhofer [39] | 0.0463 | 27.7 |
| Kastanek et al. [40] | 0.0510 | 20.4 |

Drift-flux is one of the methods to detect transition region which is based on plotting the drift flux velocity (j_{GL}) against the gas holdup (ε_G). j_{GL} is given by equation 2-1:

$$j_{GL} = \varepsilon_G (1 - \varepsilon_G) \left(\frac{U_G}{\varepsilon_G} \pm \frac{U_L}{1 - \varepsilon_G} \right) \quad (2-1)$$

where (+) sign indicate co-current flows and (-) sign means counter-current flows of the gas–liquid.

In this technique, the drift flux, j_{GL} (the volumetric flux of any phase virtual to a surface moving at the volumetric average velocity) is plotted against the superficial gas velocity, U_G .

The change in the slope of the curvature shows the transition from homogeneous flow regime to heterogeneous flow regime.

2.1.3.2 Gas holdup

The gas holdup is an important dimensionless key factor which plays a central role in the design of BCRs. It is basically defined as the volume fraction of gas in gas-liquid or gas- liquid suspension phase [24]. Similarly, the liquid and solid phase holdups are the volume fraction of liquid and solid phases, respectively.

In slurry bubble columns, the total volume (V_{Total}) of the three-phase system is given by the following expression:

$$V_{Total} = V_{Gas} + V_{Liquid} + V_{Solid} \quad (2-2)$$

As a result, the holdup of any phase, i , can be presented by the following equation [29]:

$$\varepsilon_i = \frac{V_i}{V_{Total}} \quad (2-3)$$

For three-phase SBCRs, Li and Prakash [41] put forward the following approach for measuring the gas holdup. The static pressure drop along the bed height can be calculated by:

$$\Delta P = (\rho_G \varepsilon_G + \rho_L \varepsilon_L + \rho_S \varepsilon_S) g \Delta H \quad (2-4)$$

where g , ρ , and ΔH are the gravitational acceleration, density, and height difference between the transducers, respectively. After some rearrangements, the following equation for finding the ε_G (gas holdups) is obtained:

$$\varepsilon_G = 1 - \frac{1}{g(\rho_L \phi_L + \rho_S \phi_S)} \frac{\Delta P}{\Delta H} \quad (2-5)$$

where ϕ_L and ϕ_S are volume fraction of liquid and solid phase, respectively.

The gas holdup depends on several factors: operating conditions, physical properties of the gas/liquid/solid phase, column geometry, sparger design, and solid loading. Figure 2.5 summarizes different SBCRs parameters that influence gas holdup.

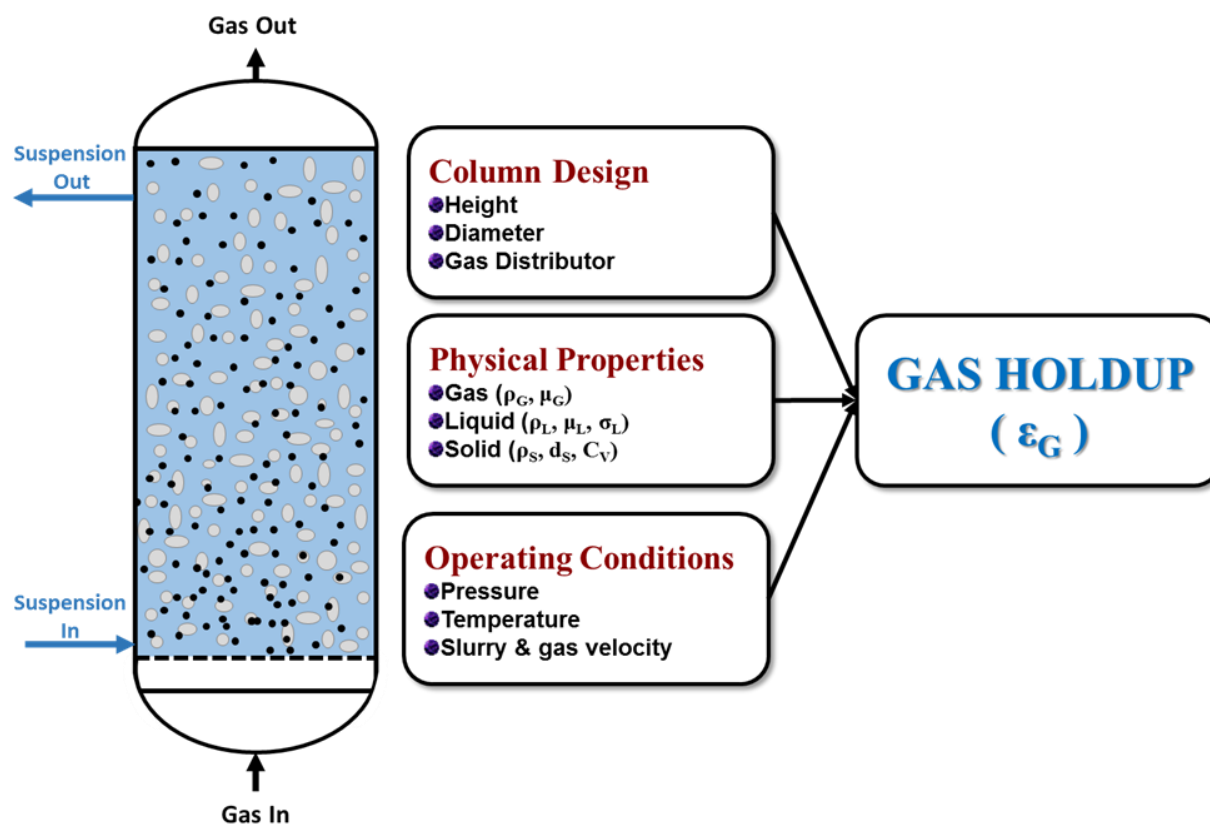


Figure 2.5- Parameters influencing the Performance of the Slurry Bubble Column Reactor.

Adapted from reference [33]

Generally, gas holdup increases with raising gas velocity and operating pressure and declines with increasing liquid viscosity and solid concentration. In bubble columns, the effect of column size on gas holdup becomes negligible as the aspect ratio reaches 5 [33]. There are a number of methods to determine the gas holdup: electroconductivity, X-ray transmission, mean resistance time distribution, optical fiber probes, particle image velocimetry, and computer tomography [42, 43]. A popular approach is plotting gas holdup against gas velocity to find the dominant flow regime. Figure 2-6 shows that with increasing gas velocity gas holdup increases and flow regime moves from the homogeneous region to the heterogeneous region [44].

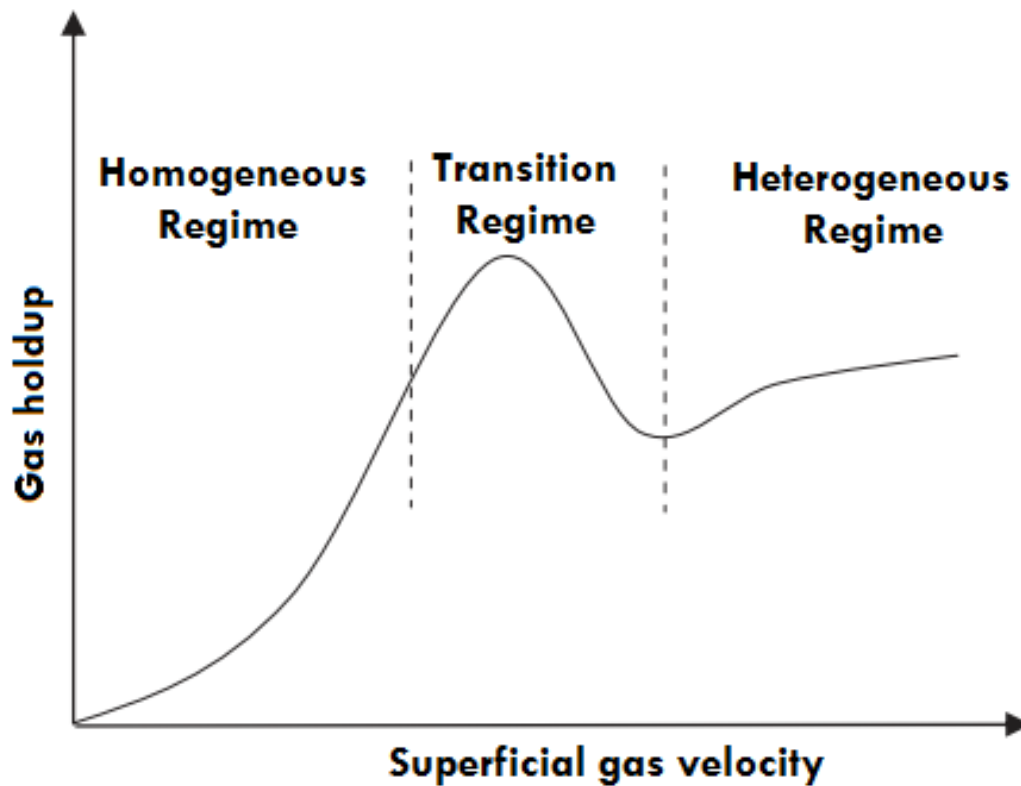


Figure 2.6- Gas holdup variation with superficial gas velocity. Adapted from reference [44]

Another method is the pressure profile method in which we basically measure the static pressure at several points (using manometers or pressure transducers) to find the pressure drop along the bed [45-48].

2.1.3.3 Superficial gas velocity

Superficial gas velocity is the average velocity of the gas that is injected into the column. This parameter can be easily calculated by dividing the volumetric flow rate by the cross-sectional area of the column. In BCRs, an increment in the superficial gas velocity leads to a rise in the gas holdup [26, 31, 41, 49-54]. This relationship is more valid for the bubbly flow regime as opposed to the churn-turbulent regime [55, 56].

2.1.3.4 Liquid phase properties

The properties of the liquid phase affect bubble formation and coalescence, which in turn has an impact on the gas holdup. In this regard, in liquids with high viscosities, larger bubbles can form which have higher rising velocities and lower gas holdup [57]. This decrease of the gas holdup in liquids with high viscosities can be attributed to either an increase in the initial bubble size or a reduction of bubble breakage due to a decrease in the collision of bubbles in a liquid result in a decrease in turbulence rate [57, 58]. In a comprehensive study with several organic liquids [59], it was indicated that the gas holdup is higher for mixtures compared to pure liquid with similar properties (surface tension, density, viscosity). Tang and Heindel [60] suggested that tap water (the most frequently used liquid in bubble columns) brings about reproducibility issues in the air–water two phase studies since the volatile compounds in tap water can influence the coalescence and subsequently the gas holdup in the column.

2.1.3.5 Solid particles

Solid particles, which usually serve as catalysts, affect the hydrodynamics and mass transfer in bubble columns. Chilekar et al. [61] analyzed this from two perspectives: (i) increase of viscosity and (ii) change in bubble coalescence due to the wetting properties in the liquid phase. The effect of solid particles on the hydrodynamics of SBCRs stems from a number of physical processes, which are elaborated below.

Density effect: Basically, due to the addition of solid particles, the density of the medium in which bubbles are rising changes. Therefore, bubble rise velocity resulting from the buoyancy alteration is influenced.

Viscosity effect: It is known that the viscosity of the slurry phase increases with solid particles concentration, size, and density [44, 62, 63]. According to the literature, viscosity can have two contradictory effects: (i) higher viscosity leads to superior bubble coalescence and lower bubble breakage, and thus gas holdup is lowered; (ii) bubble rise velocity declines at higher viscosities and thus the gas holdup increases.

Primary bubble size: Solid particles can affect bubble formation during both the expansion and the detachment stages. Variations in bubble formation can in turn influence gas holdup and regime transition.

Effect of bubble-particle interaction on bubble rise velocity: It is believed that bubble motion can be restricted by the presence of solid particles, leading to a lower rise velocity [64]. On the contrary, solid particles encourage a lateral movement of bubbles due to a collision.

Solid particles non-uniform spatial distribution: The haphazard and disordered distribution of solid particles within the column can diminish the stability of the homogeneous regime in SBCRs [65].

Regarding the influence of solid concentration and size on gas holdups, there is no general consensus. In this context, some researchers reported that increasing the solid concentration leads to an inferior gas holdup [26, 50, 52, 55, 57, 66-68]. The experiments of Kara et al. [67] and Kato et al. [66] revealed that gas holdup strongly depends on solids concentration at low especially at high gas velocities ($>10\text{--}20\text{ cm/s}$). For particle size, the phenomenon is more complicated since size effect is connected to flow regime, gas velocity and solid concentration. In one study [53], it was noted that at a fixed gas velocity and solid concentration, increasing the particle size decreased the holdup [53]. Interestingly, it was reported that unlike small gas bubbles, large bubble holdups are independent of solids concentration [50]. Li and Prakash [41, 57] observed a decrease in a holdup with solid concentration up to 25% vol. followed by a small increment at higher concentrations. This trend was ascribed to the accumulation of fine bubbles at high concentrations and a decrease in the rise velocity of small bubbles. In contrast, results of Krishna et al. [50] and de Swart et al. [69] experimental work with air-paraffin oil-glass beads three-phase system suggested that the holdup of large gas bubbles is independent of solid concentration up to 36 vol.%.

2.1.4 Dynamics of gas bubbles

The dynamics of gas bubbles are mainly influenced by the bubble size and distribution in the liquid phase throughout the column. The behavior and size of bubbles depend on the hydrodynamic flow regime, the liquid properties, reactor design, gas sparger design, and superficial gas velocity. In turn, the gas-liquid interfacial area and overall mass transfer rate strongly depend on the bubble size.

It has been suggested that in the homogeneous flow regime, bubble have narrow size distributions and there are less bubble-bubble interactions [70]. However, at higher superficial gas velocities, once we enter the churn turbulent regime, due to greater interactions between bubbles, breakage and coalescence can take place, leading to more diverse bubble sizes (generally discussed as small and large bubbles) [71]. Obviously, bubble breakage and coalescence phenomena affect both the size of the bubble and bubble rise velocity. Large bubbles rise fast and result in back mixing, while small gas bubbles move much more slowly and re-circulate within the slurry. Regarding the impact of gas flow rate on bubble size and rise velocity, Akita and Yoshida [3] observed a steady decline in bubble size with gas flow rate, while, several other researchers witnessed [41, 53, 72] appearance of a maximum bubble size upon increasing the superficial gas velocity. They also reported that generally larger bubbles present in the center of the column and smaller ones are closer to the walls. Prakash et al. [49] found that the rise velocity of small bubbles goes down with increasing the superficial gas velocity, whereas for large bubbles it follows an upward trend. Previous studies showed that the bubble size increases with liquid viscosity [57] and decreases with liquid surface tension [3]. Different from this study, Schafer et al. [73] reported that as the liquid viscosity or surface tension was reduced, the bubble diameters also dropped. Luo et al. [74] examined the influence of pressure on gas bubble properties and suggested that at a higher pressure, bubble size diminishes. This is in agreement with the study of Schafer et al. [73], in which it was indicated that higher temperature or pressure brings about smaller bubble sizes. In the presence of solids, larger bubble sizes have been evidenced by several researchers [41, 57, 74], which was ascribed to the increment in the apparent viscosity of the liquid medium.

Two phenomena significantly impact the gas bubble size and, therefore, the behavior of bubbles in SBCRs: coalescence and breakup. When two bubbles collide, a small amount of liquid is trapped

between the bubbles. During the drainage of this liquid in the next step, the liquid films on droplets are ruptured and provide the possibility for bubbles to coalesce. It is noteworthy that coalescence occurs only if sufficient time is given for the trapped liquid to reduce the film thickness. Generally, three forces account for bubble collisions: 1) turbulence from the random motion of bubbles, 2) buoyancy, and, 3) laminar shear [75]. In respect to bubble breakup, the majority of researchers applied the Rayleigh-Taylor instability or the theory of isotropic turbulence to calculate the maximum stable bubble size in the turbulent flow regime (i.e. bubble prior to breakup) [75-81]. Rayleigh-Taylor instability considers a balance between the surface tension and gravity forces acting on a gas bubble. In case the gravity force is stronger than the surface tension, the bubble will breakup. In the isotropic turbulence mechanism, the velocity fluctuations imposed by the turbulent eddies put pressures on the gas bubbles, leading to bubble deformation and finally breakup.

Different methods have been put forward to estimate bubble size, shape, and velocity [7]. Among various methods, dynamic gas disengagement technique has been used extensively to study bubble behavior in SBCRs [82]. The central idea on which this technique was built is that small and large bubbles can be distinguished if there are considerable differences between their rise velocities.

2.2 Mass transfer

2.2.1 Theories

In slurry bubble column reactors comprehensive understanding of governing mass transfer mechanism(s) and mass transfer rate across the interface between the liquid and gas phases are of paramount importance since they directly affect the design and operation of the system. In this respect, theoretical models can be helpful to describe the mass transfer phenomena and the rate. Among various theories, the two-film theory, the penetration theory, and the renewal theory are the most reliable ones which have been applied to different types of BCRs. In the following section, the main components of these theories are introduced.

2.2.1.1 Two-film theory

For mass transfer between gas and liquid, the two-phase theory is the most famous theory. This theory was first proposed by Lewis and Whitman [83] back in 1924 for gas absorption. The main pillars of this theory are: (i) absence of turbulence near the interface and (ii) mass transfer resistance is in two hypothetical films on both sides of the interface. Some of the main assumptions utilized to develop the two-film theory are listed below:

- 1) There is a film of thickness (δ) in both the gas and liquid phases, which is separated by the interface.
- 2) Mass transfer stems from the molecular diffusion within the film.
- 3) Mass transfer through the film is steady state.
- 4) The mass transfer happens at low concentrations and, therefore, the mass flux is small.

For convective mass transfer, liquid-side mass transfer coefficient is determined by equation 2-6

$$k_L = \frac{D_L}{\delta_L} \quad (2-6)$$

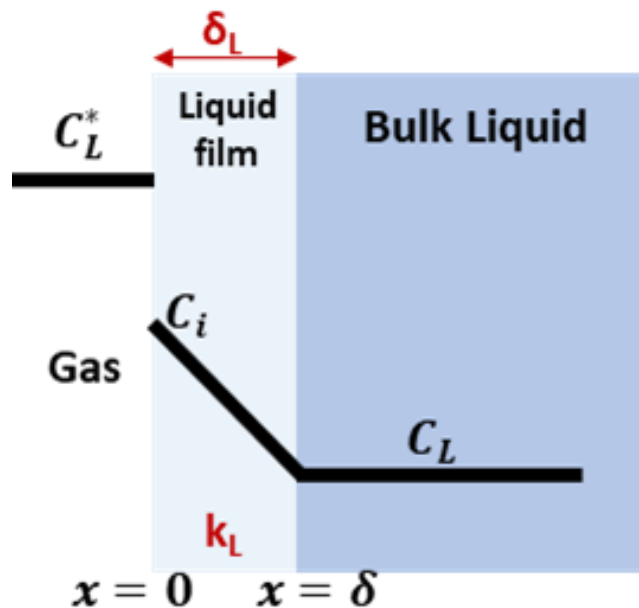


Figure 2.7- Schematic of two film theory. “Mass transfer results from molecular diffusion via the film”. Adapted from reference [83]

2.2.1.2 Penetration theory

As illustrated in Figure 2-8, the principal assumption in penetration theory (or Higbie's model) is that each liquid element is in contact with the gas for a short period of time. Put it differently, turbulent eddies move from the bulk of towards the interface, have a short residence time at the interface and result in the mass transfer, and then go back to the bulk. Furthermore, to achieve an acceptably accurate yet simple model, the following assumptions were also made:

- 1) Mass transfer from the gas to the liquid can be regarded as an unsteady state,
- 2) Each liquid element is in contact with the gas phase for the same amount of time.
- 3) There is an equilibrium state at the gas-liquid interface.

The liquid side mass transfer coefficient in terms of the contact time (θ) and the molecular diffusivity of the gas into the liquid is calculated by [5] :

$$k_L = 2\left(\frac{D_L}{\pi\theta}\right)^{0.5} \quad (2-7)$$

It should be mentioned that mass transfer is greatest for the shortest θ and for long contact times liquid side mass transfer coefficient (k_L) tends to zero.

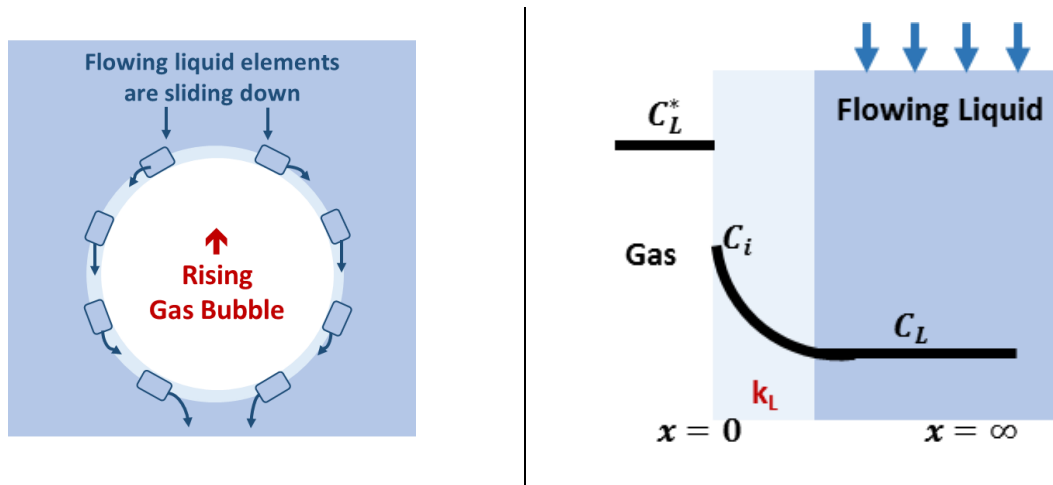


Figure 2.8- Schematic of Higbie's model. "Each liquid element is in contact with the gas phase for the same amount of time". Adapted from reference [5]

2.2.1.3 Surface-renewal theory

The foundation of the surface-renewal theory is based on the penetration theory. However, in the surface-renewal theory, a more probable (or universal) case is considered. The liquid phase is divided into two regions: the major portion of the liquid (i.e. bulk region) which is well mixed and the interfacial region. Moreover, a number of assumptions were used:

- 1) Liquid elements at the interface are replaced by new elements from the bulk
- 2) At any time, each liquid element at the interface can be replaced by a new element
- 3) Mass transfer from the gas into the liquid element is unsteady-state.

The liquid-side mass transfer coefficient in terms of the surface renewal frequency (s) and the molecular diffusivity of the gas into the liquid can be calculated by [4]:

$$k_L = (D_L s)^{0.5} \quad (2-8)$$

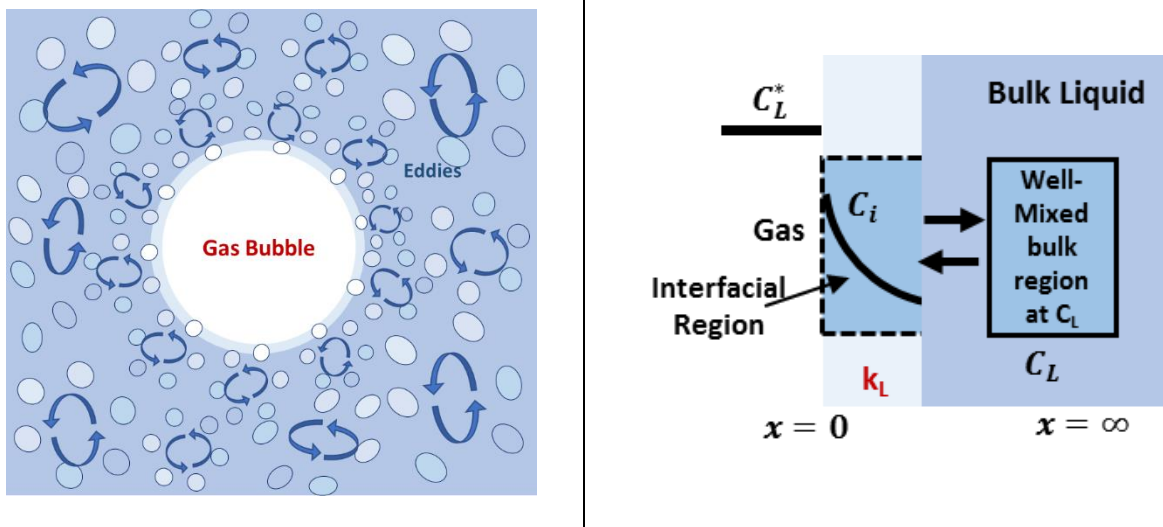


Figure 2.9- Schematic of Surface-renewal theory. “Liquid elements at the interface are randomly changed by fresh elements from the bulk”. Adapted from reference [4]

2.2.2 Volumetric mass transfer coefficient, $k_L a$

Based on previous studies [10, 14, 55, 84-97], it is logical to postulate that the total mass transport between the gas and the liquid phase in SBCRs is controlled by the mass transfer from the gas-liquid interface to the bulk liquid. Consequently, we need to determine the liquid-side mass transfer coefficient (k_L) and the gas-liquid interfacial area (a).

In a unit volume of a BCR, gas holdup made up of n bubbles can be expressed by the following equation (assuming spherical bubble with diameter d_b):

$$\varepsilon_G = \frac{V_G}{V_{Total}} = \frac{n \left(\frac{\pi d_b^3}{6} \right)}{V_{Total}} \quad (2-9)$$

The interfacial area in the unit volume is defined as

$$a = \frac{\text{Total surface area of bubbles}}{\text{Total volume}} = \frac{n(\pi d_b^2)}{V_{Total}} \quad (2-10)$$

Combining these two expressions (2-9) and (2-10), equation (2-11) provides the specific interfacial area [34]:

$$a = \frac{6\varepsilon_G}{d_b} \quad (2-11)$$

Therefore, the specific interfacial area is a function of gas holdup and bubble size. Having small bubbles in the reactors and large gas holdup lead to a high gas-liquid interfacial area, in other words, good interphase contacting between phases.

Despite the fact that there are numerous articles on the overall volumetric mass transfer coefficient, only a handful of works have been dedicated to the study of k_L and interfacial area separately in slurry bubble column reactors [98, 99]. This limits our understanding of dominant gas-liquid mass transfer mechanisms.

Finding the liquid-side mass transfer coefficient, based on the equation presented in sections 2.2.1.1-2.2.1.3, necessitates the knowledge of the gas-liquid diffusivity (D_L) and the liquid film thickness (δ) or contact time (θ) or surface renewal frequency (s), depending on which mechanism is dominant. The diffusivity can be found in available literature correlations, however, the

measurement of δ , θ and s can be a challenging task. Table (2-2) lists previous studies that focused on measuring k_L and interfacial area.

Table 2.2- Correlations for predicting (a) and (k_L) in BCs and SBCs

| Researchers group | Model prediction |
|-----------------------------|---|
| Akita & Yoshida (1974) [3] | $k_L = 0.5g^{0.625}\rho_L^{0.375}\sigma_L^{-0.375}D_L^{0.5}d_{vs}^{0.5}$ |
| Godbole et al. (1984) [100] | $k_L = 1.12 \times 10^{-4}U_G^{-0.03}\mu_L^{-0.5}$ $a = 19.2U_G^{0.47}\mu_L^{-0.76}$ |
| Miyahara et al. (1997) [2] | $k_L = 2 \times 10^{-4}\left(\frac{\mu_L}{\rho_L D_L}\right)^{0.5}\left(\frac{\rho_L U_G d_s}{\mu_L}\right)^3\left(\frac{g\mu_L^4(\rho_L - \rho_G)}{(\rho_L^2 \sigma_L^3)}\right)^{0.45}\frac{D_L}{d_s}$ $a = 24.37\varepsilon_G^{0.973}\sigma_L^{-0.766}\mu_L^{-0.192}, 2 - Phase$ $a = 35\varepsilon_G^{0.973}\sigma_L^{-0.766}\mu_L^{-0.192}, 3 - Phase$ |
| Neme et al. (1997) [101] | $k_L = 0.105U_G(ReFrSc^2)^{-0.268}, 2 - Phase$ $k_L = 0.103U_G(ReFrSc^2)^{-0.265}, 3 - Phase$ |
| Schumpe et al. (1987) [88] | $k_L = 9.7 \times 10^{-5}U_G^{-0.05}\mu_L^{0.15}, (H_2O/Salt\ Solution)$ $k_L = 6.45 \times 10^{-5}U_G^{-0.05}\mu_L^{0.15}, (H_2O/0.8M\ Na_2SO_4)$ |
| Tomida et al. (1978) [102] | $a = 4.65 \times 10^{-12}\left(\frac{U_G}{\mu_L}\right)^{0.51}$ |
| Vázquez et al. (2000) [1] | $k_L = 0.17587 U_G^{0.5}\sigma_L^{1.35}, (d_{BPPS} = 150 - 200\ \mu m)$ $k_L = 0.18233 U_G^{0.5}\sigma_L^{1.35}, (d_{BPPS} = 90 - 150\ \mu m)$ $k_L = 0.18689 U_G^{0.5}\sigma_L^{1.35}, (d_{BPPS} = 40 - 90\ \mu m)$ |

Several works have been devoted to the investigation of the effect of operating conditions and solid concentration on $k_L a$. For instance, $k_L a$ improves with increasing the superficial gas velocity, gas density and operating pressure while it deteriorates with liquid viscosity. Behkish et al. [103] showed that at higher solid concentrations, volumetric mass transfer coefficient possesses lower values. They justified this behavior by pointing out that upon addition of solids, the bubble coalescence leads to the formation of larger bubbles and thus decrement in the interfacial area [103].

Similarly, Kim et al. [104] observed that $k_L a$ value increased by using Al_2O_3 nanoparticles at low concentrations due to the bubble breakage effect. However, at higher solid concentrations (i.e. higher liquid viscosity), the formation of larger bubbles is facilitated due to the coalescence. Vandu and Krishna [10] developed a model for high slurry concentrations and high superficial gas velocities (0-40 cm/s) in bubble column at ambient conditions and revealed that volumetric mass transfer coefficient is mainly dependent on the gas holdup.

2.2.2.1 Oxygen transfer from air bubbles into the water

Transfer of one component such as oxygen from the air bubble (gas phase) into the water (liquid phase) has several steps and resistances. It is widely accepted that the resistance associated with the liquid film encompassing the gas bubbles contributes the most to the overall mass transfer resistance. In this context, the two film model has been applied by many researchers to investigate the gas-liquid mass transfer. A schematic representation of different stages of mass transfer according to the two-film theory is brought in Figure 2-10.

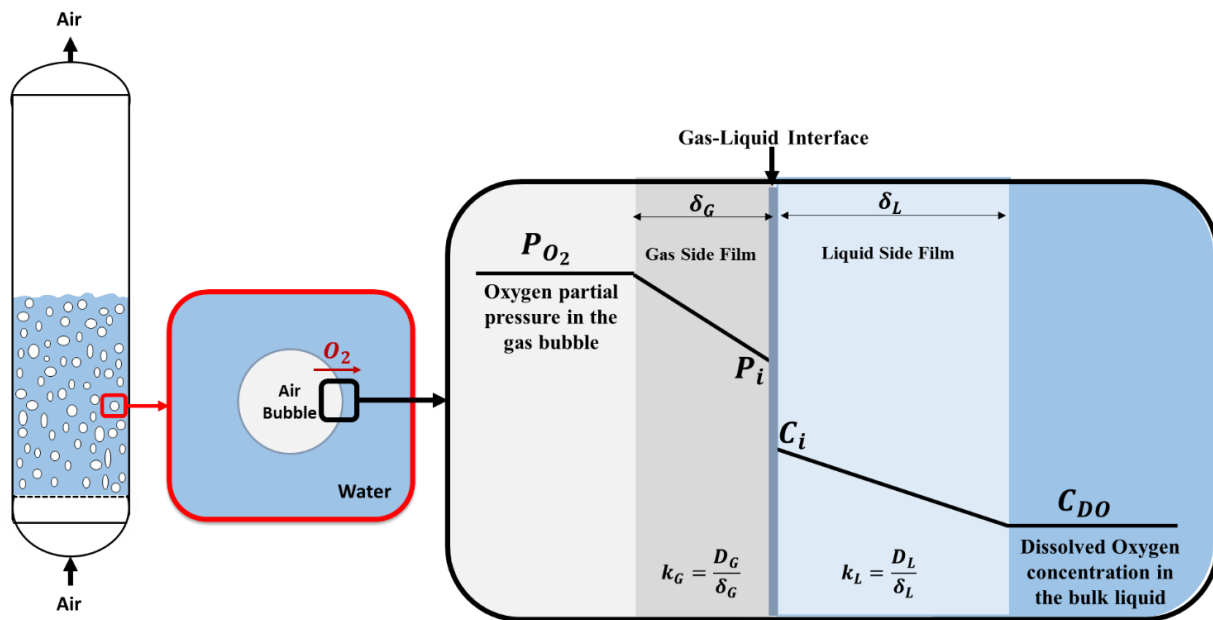


Figure 2.10- Sketch of oxygen transfer from the air bubble into the water based on two film theory. Adapted from reference [83]

As can be seen in this figure, the mass flux in each film can be calculated by multiplying the concentration difference (i.e. the driving force) by the mass transfer coefficient.

$$J_{O_2} = k_G(P_{O_2} - P_i) = k_L(C_i - C_{DO}) \quad (2-12)$$

Where J_{O_2} is the molar flux of oxygen $\left(\frac{\text{mol}}{\text{m}^2\text{s}}\right)$, and k_L and k_G are the local mass transfer coefficients. P_{O_2} and P_i are oxygen partial pressures in the air bubble and the gas-liquid interface, respectively. Similarly, C_{DO} and C_i are the dissolved oxygen concentrations in the bulk liquid and the interface, respectively.

Considering the fact that the interfacial concentrations cannot be directly measured, the above equation should be rewritten as:

$$J_{O_2} = K_G(P_{O_2} - P_{O_2}^*) = K_L(C_{O_2}^* - C_{DO}) \quad (2-13)$$

where $P_{O_2}^*$ is the oxygen pressure in equilibrium with the liquid phase, $C_{O_2}^*$ is the oxygen saturation concentration (calculated by Henry's law, $P_{O_2}^* = HC_{O_2}^*$) in the bulk liquid in equilibrium to the bulk gas phase, and K_G and K_L are the overall mass transfer coefficients.

If we combine these two equations (2-12 and 2-13), we reach the following correlation:

$$\frac{1}{K_L} = \frac{1}{k_L} + \frac{1}{Hk_G} \quad (2-14)$$

Considering the fact that the oxygen solubility in water is small (so H is very large), it is logical to neglect the second term in equation 2-14, and only consider the resistance in liquid side of the interface. Consequently, the overall mass transport coefficient will be equal to the local coefficient:

$$K_L = k_L.$$

In SBCR, the oxygen mass transfer rate per unit volume, N_{O_2} , can be expressed as:

$$N_{O_2} = a \cdot J_{O_2} = k_L a (C_{O_2}^* - C_{DO}) \quad (2-15)$$

In this equation, the overall flux (which is mol/s per surface area) is multiplied by the gas-liquid interfacial area (which is surface area per unit of liquid volume) to obtain molar flowrate per unit volume.

2.2.3 Mass transfer measurement techniques

In SBCRs, one of the key obstacles against an accurate estimation of mass transfer is measuring local concentrations. In order to determine the gas-liquid interfacial area and mass transfer coefficient in multi-phase systems, the measurement techniques can be mainly divided into direct methods and indirect methods [15]. In direct methods, the diffusion coefficient is assessed by measuring the concentration of diffusing species as a function of depth of penetration [105]. Radioactive tracer technique, mass spectrometry, and spectrophotometry are among the most

common direct physicochemical methods. It is to be noted that despite the fact that direct methods are very reliable, they are also costly, time-consuming and intrusive.

In indirect approaches, changes in one of the system parameters that are dependent on the diffusion rate are tracked to calculate the diffusion coefficient. In this context, the rate of change of solution volume, the rate of pressure-drop in a confined cell, the rate of gas injection from the top to a cell (in which pressure and solution volume are fixed), and magnetic field characteristics are the most widely applied parameters. Unlike the direct methods, with indirect approaches, it is not necessary to measure the variations in the chemical composition of phases. Some of the well-known approaches are: pressure decay, magnetic resonance imaging, CAT scanning, and low field NMR, and dynamic pendant drop shape analysis [106-111].

CHAPTER 3 EXPERIMENTAL AND METHODOLOGY

3.1 Materials

Oil – free air supplied by a central compressor is used as the gas phase. The flow rate of air is controlled by two rotameters, which allow operating in both homogeneous and heterogeneous flow regimes. The superficial gas velocity can be varied from 0.4 cm/s to 25 cm/s . Nitrogen is also employed as a gas phase as well in the saturation method to remove dissolved oxygen in the liquid medium.

Tap water serves as the liquid phase in all experiments which are being operated in batch mode (only gas flows upward). Glass beads are used in the column as the solid phase to obtain the slurry phase. It is to be noted that the experiments are conducted in the semi- batch mode. Prior to the addition of solid phase (i.e. glass beads) to the liquid, the initial height of liquid in the column is 1.10 meter. Two different sizes of hydrophilic glass beads are employed: $71 \mu\text{m}$ and $156 \mu\text{m}$, both having a density of 2500 kg/m^3 . The volume fractions (C_V) of solid particles in the liquid phase are: 0, 1, 3 and 5 %.

Table 3.1- Physical properties of materials in this work

| Physical properties (20°C) | | | |
|-----------------------------------|-------------|---|---|
| Gas: | Air | $\rho_G = 1.225 \text{ (kg/m}^3\text{)}$ $\mu_G = 1.83 \times 10^{-5} \text{ (kg/(m.s))}$ | |
| Liquid: | Tap water | $\rho_L = 997.04 \text{ (kg/m}^3\text{)}$ $\mu_L = 0.001002 \text{ (kg/(m.s))}$ $\sigma_L = 0.0729 \text{ (N/m)}$ $D_L = 2.56 \times 10^{-9} \text{ (m}^2\text{/s)}$ | |
| Solid: | Glass beads | $\rho_S = 2500 \text{ (kg/m}^3\text{)}$ $C_V = 0, 1, 3, 5\%$ | |
| | | d_P | |
| | | $71 \mu\text{m}$ | 10% finer than 59 (μm) and 90% finer than 85 (μm) |
| | | $156 \mu\text{m}$ | 10% finer than 125(μm) and 90% finer than 192(μm) |

3.2 Experimental Setup

Figure 3.1 shows a schematic of the experimental set up used to study the volumetric mass transfer coefficient in the slurry bubble column in this work. All experiments are carried out in a Plexiglass slurry bubble column of 2.61-meter total height and 0.292-meter inner diameter. The gas distributor is a perforated plate which has 94 holes of 1 mm orifice diameter with 1400 holes/m² density.

To measure the dissolved oxygen concentration in the liquid phase, an optical dissolved oxygen (DO) probe (Visiferm DO325, Hamilton Inc.) is used. The DO probe is located 0.55 m above the distributor. The probe's range of measurement for dissolved oxygen is 4 ppb to 25 ppm. The probe has 0.012-meter diameter and 0.325-meter length. For all 2-phase experiments, the DO concentration is determined at seven radial positions, while in the case of 3-phase experiments only the DO concentration at the center of the column is measured. This optical probe is worked on the basis of oxygen dependent luminescence quenching.

To record dynamic dissolved oxygen concentration and temperature of media, one data acquisition card (National Instrument, PCI6023E) and LabVIEW software are used. All data are recorded for 180 s and 512 Hz frequency. Each experiment is done for three times for 3-phase and five times for 2-phase to ensure repeatability and the mean average of obtained data in these tests are presented as the final results.

Table 3.2- Operating conditions and geometrical specifications of the BC with distributor

| <i>Column dimension</i> | |
|------------------------------------|--|
| D_C | 0.292 (m) |
| H_C | 2.61 (m) |
| H_0 | 1.10 (m) |
| Gas distributor | Perforated plate $d_0 = 1$ (mm) (94 holes) |
| <i>Operating conditions</i> | |
| P | 1 (atm) |
| T | 15 – 22 (°C) |
| U_G | 0.004– 0.25 (m/s) |

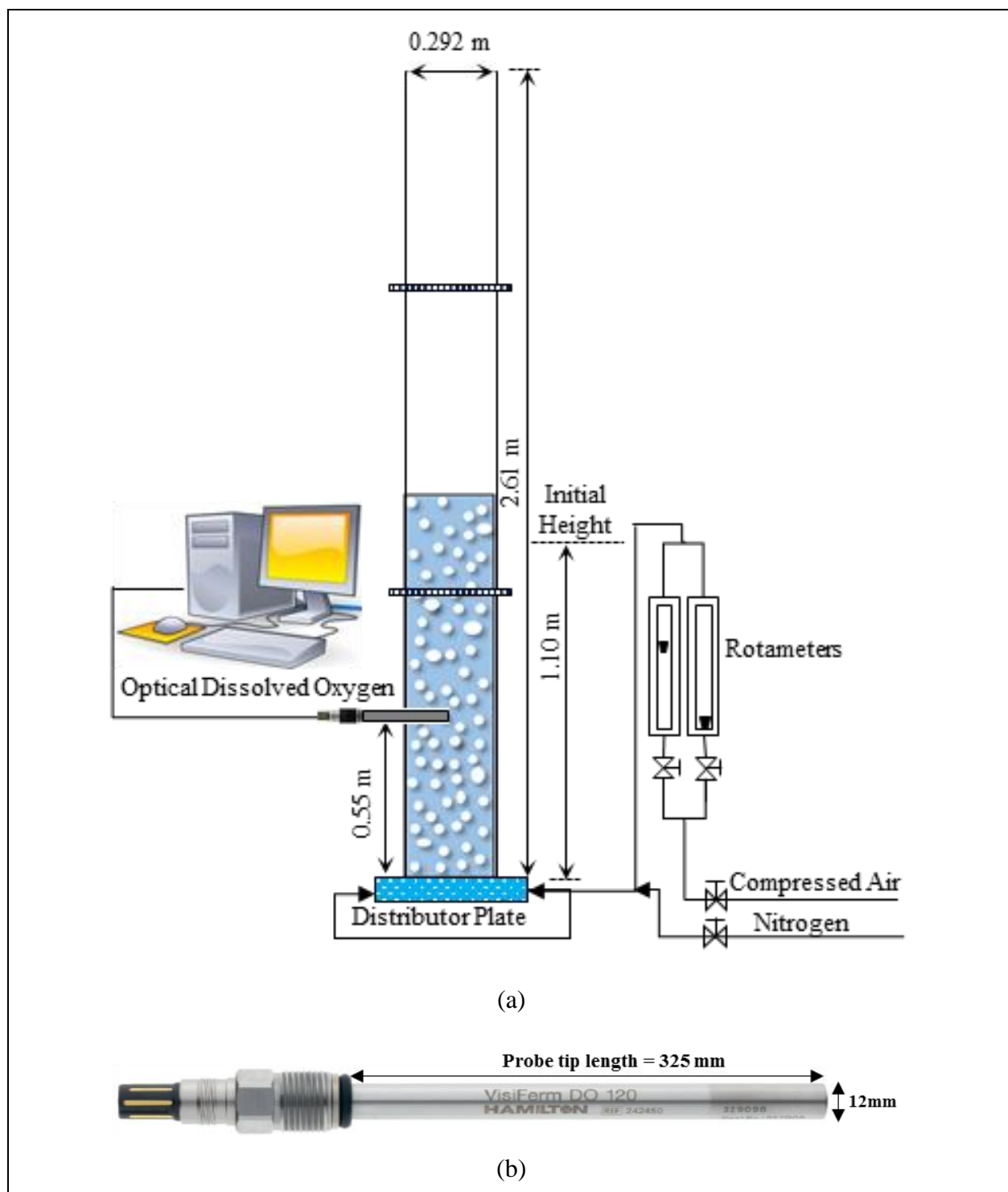


Figure 3.1- (a) Schematic of experimental set-up (b) Photograph of optical dissolved oxygen probe (VisiFerm DO325, Hamilton Inc.)

3.3 Measurement of volumetric mass transfer coefficient

In order to determine the volumetric liquid-gas mass transfer ($k_L a$), the dynamic oxygen absorption technique has been utilized. Among the different methods available for this technique, the saturation method has been applied in this study. Regarding the details of the saturation method, in the first step, nitrogen is introduced into the column in order to bring the concentration of dissolved oxygen to nil. In the next step, the nitrogen flow is stopped, allowing all N_2 bubbles to leave the liquid phase. Subsequently, pressurized air is sparged into the column and the concentration of dissolved oxygen is continuously measured via the optical probe.

Assuming that the liquid is perfectly mixed and the oxygen depletion from the gas bubble is insignificant, by considering a simple mass balance for dissolved oxygen as follows the concentration of DO at each moment can be calculated.

$$\frac{dC}{dt} = k_L a (C^* - C) \quad (3-1)$$

In this equation C^* is the oxygen solubility (i.e. oxygen saturation concentration at the liquid-gas interface) at employed temperature and pressure, and C is the oxygen concentration in the liquid phase.

Considering that the concentration of DO at t_0 (the starting point of the experiment) is equal to zero, the integration of the above equation results in [112] :

$$C(t) = C^* [1 - \exp(-k_L a (t - t_0))] \quad (3-2)$$

The only unknown constant in this equation is the volumetric mass transfer, which can be found by a regression of Equation 3-2 to the actual concentration of $C(t)$ read by the probe [14] .

CHAPTER 4 RESULTS AND DISCUSSION

4.1 Effect of superficial gas velocity

As highlighted throughout the literature review section, superficial gas velocity is an important parameter in SBCRs since it not only controls the flow regime, but also affects the gas holdup, gas bubbles characteristics, and mass and heat transfer. Figure 4.1 illustrates the variations in the dissolved oxygen concentration versus time for the air-water system at three different superficial gas velocities ($U_G = 0.56, 5.28$ and 18.55 cm/s).

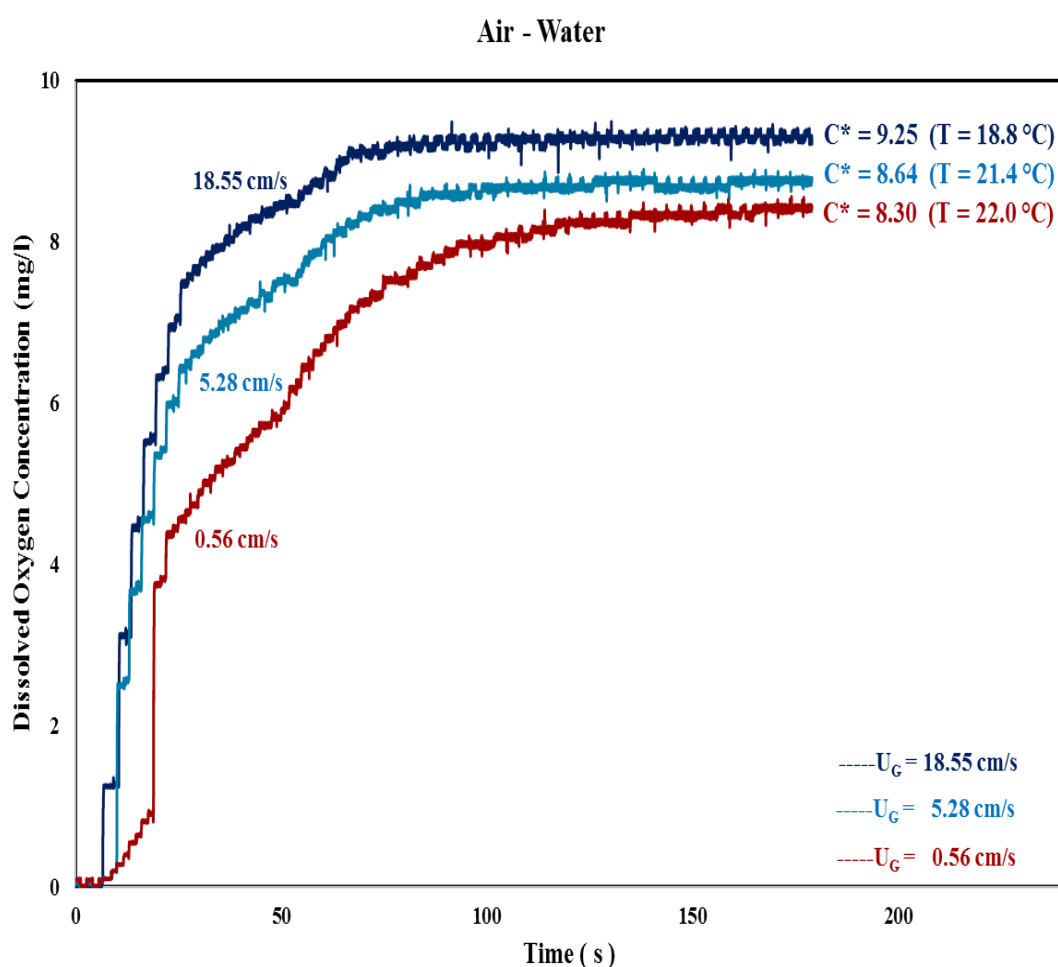


Figure4.1- Dissolved oxygen concentration variation for air–water system.

For all gas velocities, the DO concentration-time profile can be divided into three distinct regions, which are elaborated below. At the beginning (time span of 0 to 10 s), the dissolved oxygen concentration is nearly constant. In the second stage, dissolved oxygen concentration increases with time very sharply in less than 15 s. This is followed by a less noticeable increment in DO with time between 25 and 65 s. Finally, DO reaches a plateau, where DO concentration is independent of the time of the experiments. Interestingly, it was noticed that the temperature drops as the superficial gas velocity is raised, which can be attributed to the following facts. Considering the fact that the temperature of the compressed air is lower than that of the liquid phase (i.e. tap water), as the air flowrate is increased, the temperature of the air-water system goes down. Additionally, at higher air velocities, more water evaporation rates can be envisaged, leading to the temperature drop.

Nevertheless, it needs to be emphasized that in each test (at each superficial gas velocity), the DO concentrations are recorded in a constant temperature.

As the superficial gas velocity is raised, more severe mixing in the system can be expected, which results in better contact between the liquid and gas phases. Based on the surface renewal theory, the superior contact between the two phases enhances the mass transport rate. Therefore, at higher gas velocities, the dissolved oxygen reaches its saturation concentration (i.e. equilibrium state) sooner. This can be easily deduced from: i) the steeper slope for $U_G=18.55$ cm/s with respect to that at 0.56 cm/s (or 5.28 cm/s) in Figure 4.1, and ii) the significant difference in the required time to reach the saturation concentration (60, 80, and 130 s for 18.55, 5.28, and 0.56 cm/s, respectively).

In order to confirm the accuracy of the data obtained by the DO probe, the saturation concentration of dissolved oxygen at different temperatures were recorded and compared to those reported in the literature (presented in Table 4.1). As the water temperature increased, lower saturation DO concentrations were seen for the air-water system. As can be noted from Table 4.1, the obtained values for saturation DO concentration in the present work are acceptably close to those reported by Weiss et al.[113], validating the reliability of the applied methodology and the exploited measurement technique.

Table 4.1- Solubility of oxygen in water at various temperatures and atmospheric pressure.

(MAPE = 1.3 %)

| Temperature (°C) | Saturation DO | |
|-------------------------|----------------------|-------------------------------------|
| | Present Work | From R.F. Weiss (1970) [113] |
| 17.0 | 9.64 | 9.6 |
| 17.5 | 9.54 | 9.5 |
| 18.0 | 9.44 | 9.4 |
| 18.5 | 9.32 | 9.3 |
| 19.0 | 9.21 | 9.3 |
| 19.5 | 9.11 | 9.2 |
| 20.0 | 9.01 | 9.1 |
| 20.5 | 8.89 | 9 |
| 21.0 | 8.76 | 8.9 |
| 21.5 | 8.62 | 8.8 |
| 22.0 | 8.30 | 8.7 |

4.2 Radial distribution of volumetric mass transfer coefficient

Figure 4.2 displays the volumetric mass transfer coefficient in the air-water system at different radial positions for two superficial gas velocities (0.4 and 21.3 cm/s). As can be seen in this figure, under both low and high gas velocities, the variations in the mass transfer coefficient in the radial direction are not considerable.

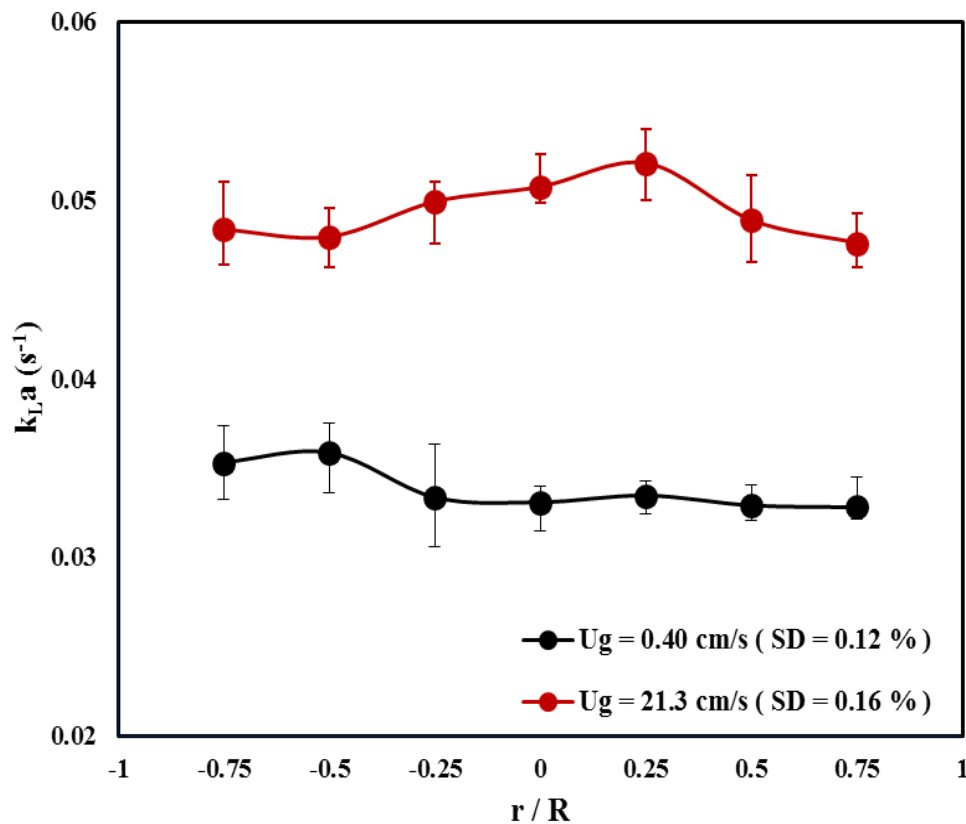


Figure 4.2- Radial distribution of volumetric mass transfer coefficient in the air-water system.

The standard deviation for $k_L a$ is calculated based on the following formulae (Equation 4.1):

$$SD = \sqrt{\frac{\sum \left(k_{La} \left(\frac{r}{R} \right) - k_{La}^{Average} \right)^2}{n-1}} \quad (4-1)$$

Taking into consideration the results for $k_L a$ for different radial positions (Figure 4.2) and their standard deviations, it is reasonable to suggest that at each cross section of the column (i.e. same

column height) the $k_L a$ is similar in the radial direction and this coefficient only changes with height the of the column. Our results are also in good accordance with previous findings, in which the changes in the mass transfer coefficient in the radial dispersion were considered insignificant [114, 115]. This was mainly ascribed to the rapid liquid phase mixing in the SBCRs.

The above-mentioned behavior was, in fact, valid for all tested gas velocities, as depicted in Figure 4.3.

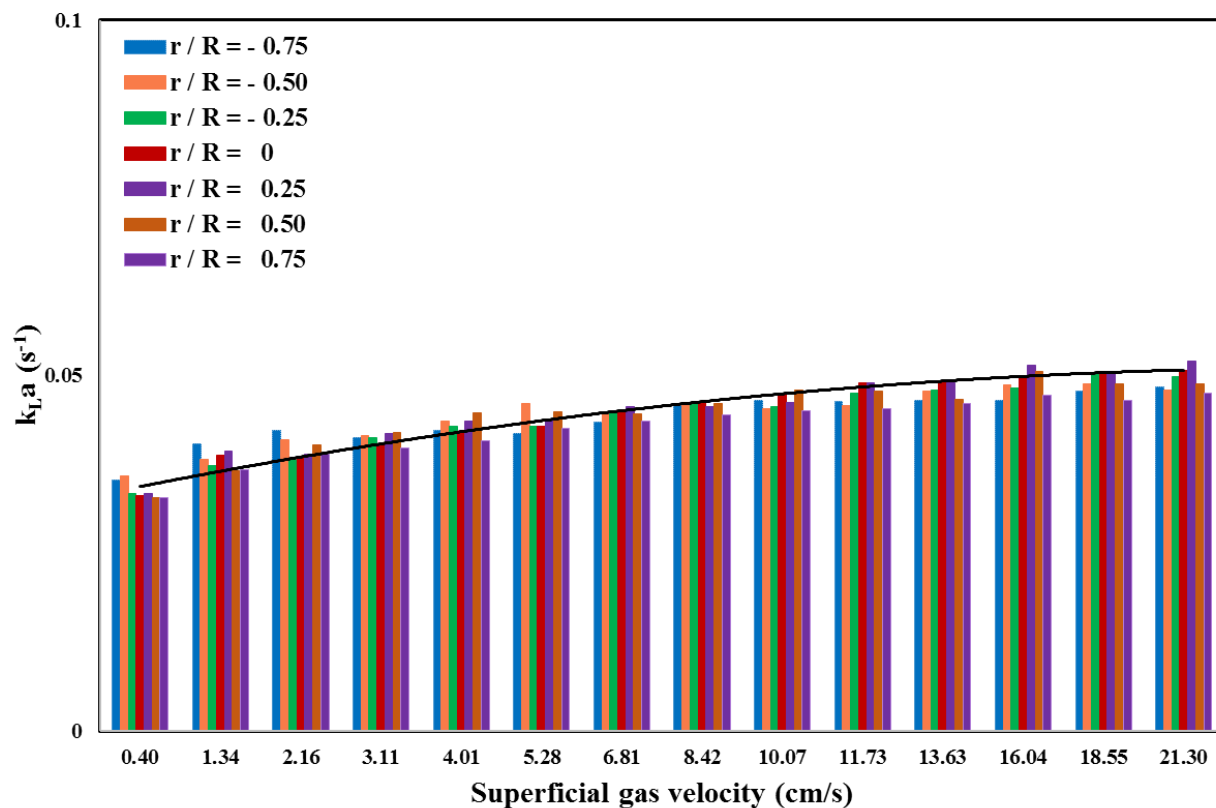


Figure 4.3- Radial distribution of $k_L a$ in the air-water system.

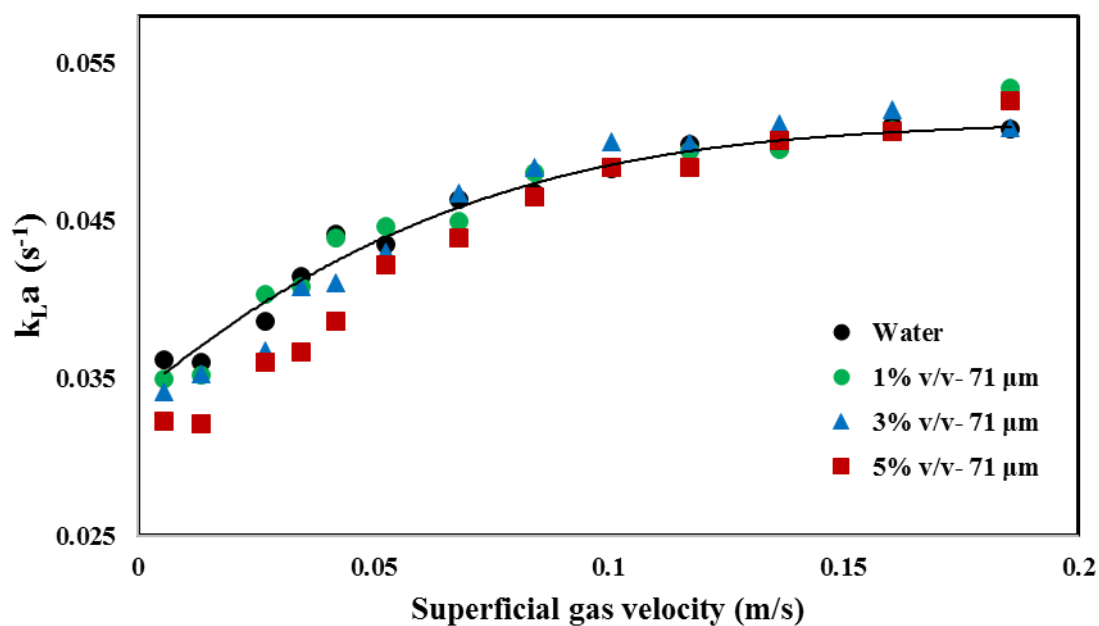
Figure 4.3 shows that with increasing the superficial gas velocity the mass transfer coefficient improves; however, similar to Figure 4.2, the differences in $k_L a$ in the radial position are negligible. Considering these observations in the two-phase system, for our experiment with the three-phase system, the mass transfer coefficient was determined on for the center of the column.

4.3 Effect of solid concentration

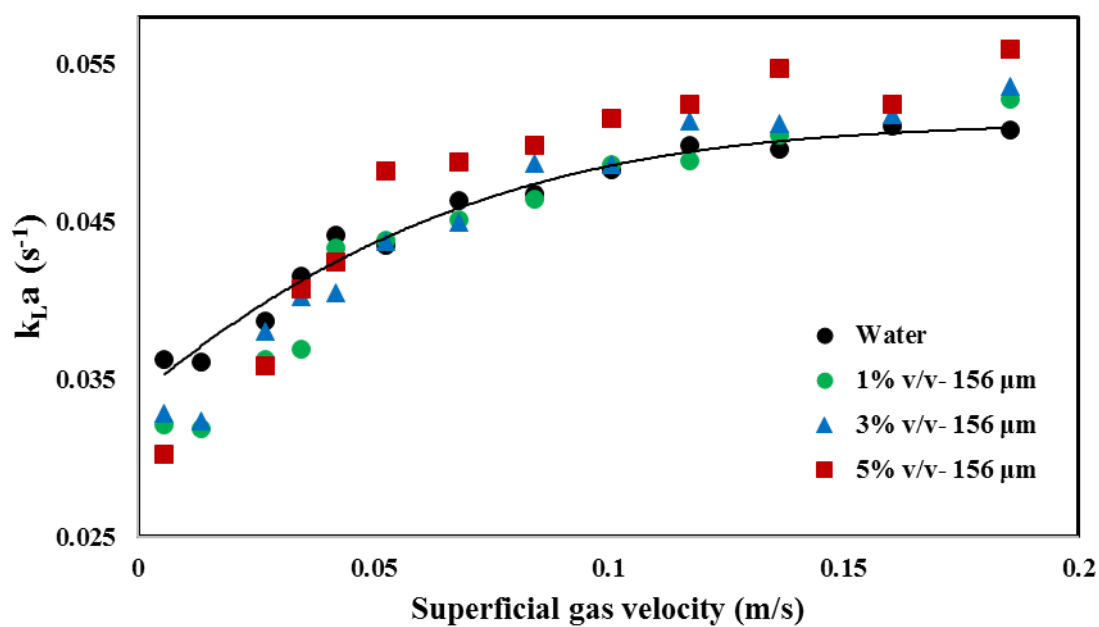
As mentioned in section 2.1.3.6, both solid particles size and concentration can exert influence on the mass transfer in slurry bubble column reactors. In order to explore this influence, the variations in mass transfer coefficient with superficial gas velocity were assessed at four solid concentrations (0 (two-phase system), 1, 3, and 5% v/v) and two different particle sizes (71 and 156 μm). Figure 4-4a and 4-4b present the dependence of $k_L a$ on superficial gas velocity in systems with 71 μm and 156 μm glass beads as the solid phase.

Black trendlines in both figures show the relationship between the two parameters (i.e. $k_L a$ and gas velocity) in the two-phase air-water system. As can be seen in Figure 4-4, by increasing the superficial gas velocity the mass transfer coefficient steadily improves, which can be explained from two perspectives. First, as the superficial gas velocity is raised, the gas holdup increases as well, leading to enhanced mass transfer. Additionally, as it was discussed in section 2.2.2, considering the equation (2-11), by increasing the gas holdup (ε_G), the gas-liquid interfacial area increases as well, which in turn clearly elevates the magnitude of mass transfer. On the other hand, at higher gas velocities, a more turbulent flow regime can be expected. Based on the discussions about the surface renewal theory, it is known that as the mixing (or turbulence) is augmented, gas-liquid contact time is shortened; therefore, the mass transfer rate between the two phases is improved.

Another interesting observation in these experiments is the difference in the behavior of two-phase and three-phase systems to increment in superficial gas velocity. The effect of solid particles on $k_L a$ can be divided into two regions according to the gas velocity. In low gas velocities, it can be noted that the presence of solids particles negatively affected the mass transfer, while, on the contrary, at high velocities, solids particles possess a promoting effect.



(a)



(b)

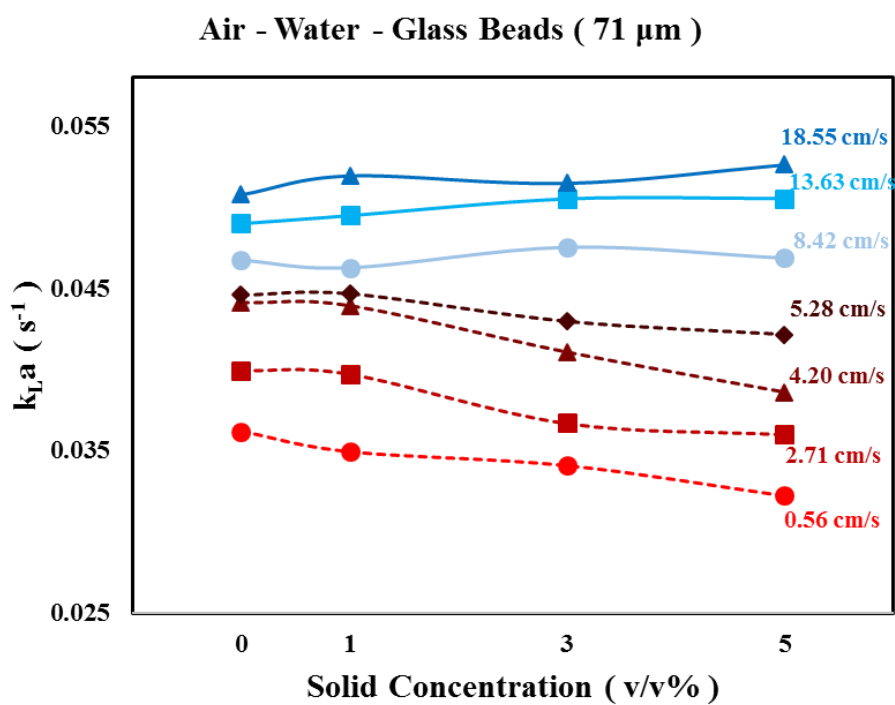
Figure 4.4- Impact of U_G on the $k_L a$ - (a) Air-Water-Glass beads 71 μm - (b) Air-Water-Glass beads 156 μm

Figure 4-5 illustrates the impact of glass-bead particles concentration on the $k_L a$ at different superficial gas velocities and two solid particles sizes.

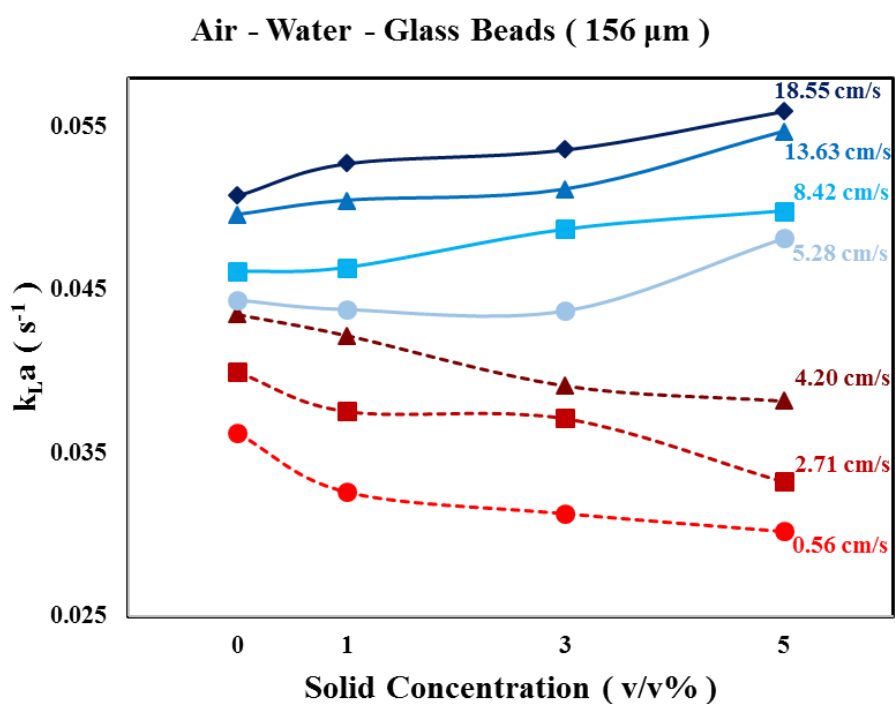
Similar to the behaviors noted in Figure 4-4, at low gas velocities solid particles inhibited the gas-liquid mass transfer, while at high velocities, employing the solid phase resulted in a superior mass transfer. Moreover, the improvement in the mass transfer coefficient (at high velocities) upon applying the solid phase is more noticeable for 156 μm particle size system with respect to that for 71 μm .

The influence of solids particles on the mass transfer processes can be analyzed from different angles. The decrement in the mass transfer coefficient with solid concentration at low velocities can be justified by taking into consideration the following points:

- The glass beads utilized in this study is hydrophilic. According to the literature, hydrophilic solids particles in slurry bubble column reactors can adversely affect the gas holdup. Considering the direct relation between the gas holdup and the gas-liquid interfacial area, as gas holdup goes down with increasing the concentration of solid particles, the interfacial area and consequently the volumetric mass transfer diminish.
- With adding solid particles to the system, the viscosity of the fluid increases, which in turn decreases the diffusion coefficient (D_L). Given the fact that k_L is directly related to the diffusion coefficient, at higher solid concentrations, k_L declines.
- Solid particle size and concentration affect the gas bubble size as well. Since fluid viscosity is higher at higher solids concentration, the system allows the formation of larger gas bubbles. Clearly, as the gas bubble size increases, a smaller interfacial area can be achieved according to equation 2.11 and the overall mass transfer rate goes down.
- Formation of larger gas bubbles at higher solid concentrations can also lead to a more bubble rise velocity. Naturally, at higher velocities, the residence time of gas bubbles within the fluid shortens, reducing the $k_L a$.



(a)



(b)

Figure 4.5- Impact of solid particles concentration on the $k_L a$ at different U_G -(a) Air-Water-Glass beads 71 μm , (b) Air-Water-Glass beads 156 μm

The improvement in the mass transfer coefficient in the system with glass beads at high velocities can be explained as follows. Hindering effect: Solids particles may induce the collision phenomenon in the column which lowers the rising of bubbles and increases the probability of contact between bubbles and liquid, which consequently enhances the mass transfer. However, the behavior of the system at low and high superficial gas velocities is different. At low velocities, a main fraction of the solid particles settled at the bottom of the column, this can lead to the formation of gas bubbles with a larger initial size, which is obviously undesirable in terms of interfacial area. As the gas velocity is raised, the distribution of solid particles (i.e. glass beads) in the column becomes more uniform and smaller gas bubbles are produced. Moreover, at higher velocities, the breakage phenomenon comes to play due to the strong impact between the solid particles and gas bubbles. This process breaks up large bubble into smaller ones which can offer a larger interfacial area and improve $k_L a$. In addition, it is postulated that due to their higher inertia, larger glass beads might deviate more from the liquid streamlines compared to the smaller ones; therefore, a greater collision can be envisaged. This led to a more significant rise in the mass transfer coefficient with solid concentration for 156 μm particles.

4.4 Effect of particle size

In Figure 4-6, the ratio between the mass transfer coefficient for the 3-phase system and that of the 2-phase one ($\frac{k_L a}{(k_L a)_0}$) is depicted for two particle sizes (71 and 156 μm) at different gas velocities.

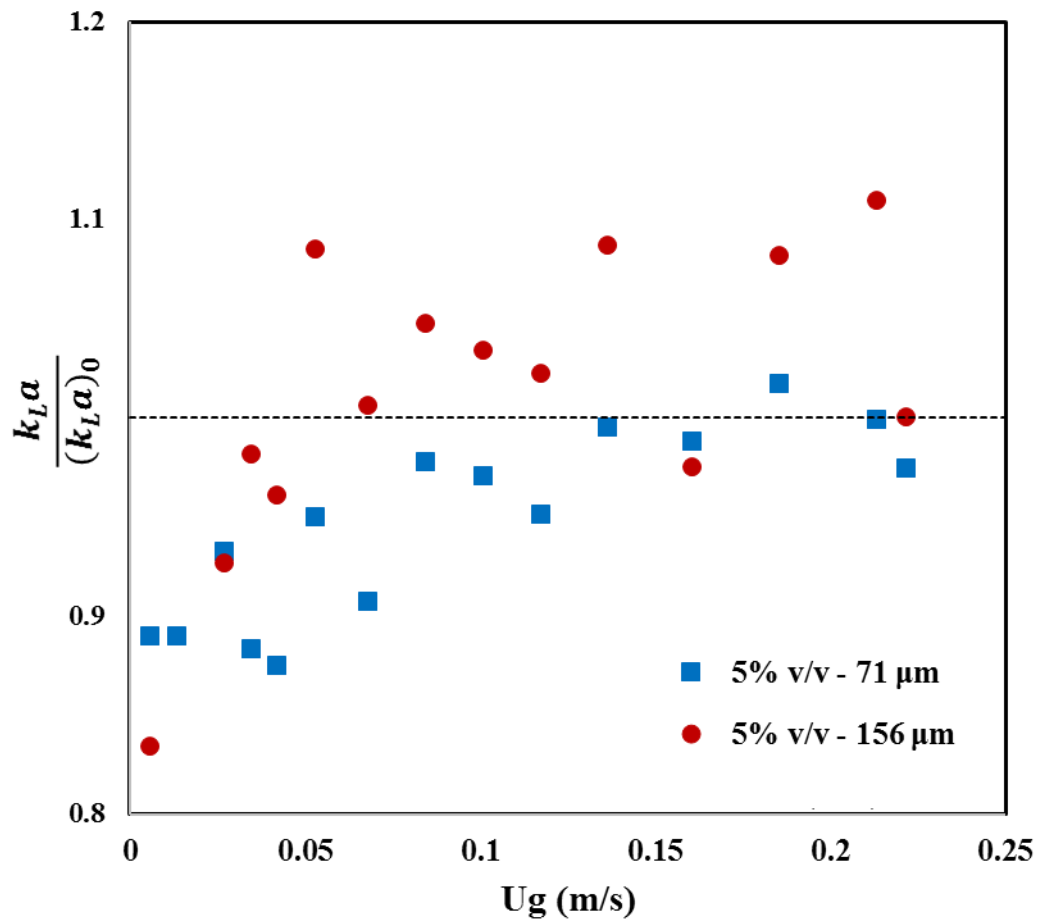


Figure 4.6- Effect of particle size on $k_L a$ at a constant solid concentration

It should be mentioned that for all the data points in this figure, the concentration of the solid phase is 5%. This graph clearly indicates the interconnection between the particle size and superficial gas velocity and its net effect on the mass transfer coefficient. As highlighted before, the presence of solid particles especially at high velocities results in bubble breakage and larger interfacial area. As can be seen in this figure, for most gas velocities, using the larger size glass beads (i.e. 156 μm),

brought about a considerable enhancement in the mass transfer coefficient, mainly due to the bubble breakage and enlargement of the surface area. The dashed line in this figure represents a situation in which there is no difference between the mass transfer in the two and three-phase systems. As can be noted, most of the blue squares fall below the line, meaning that utilizing solid particles at low gas velocity is solely inhibiting.

4.5 Developing a new model for predicting $k_L a$

In the past years, many researchers have studied the performance of slurry bubble columns; however, the majority of these works have been focused on the laboratory scale testing. Considering this, it is of great importance to establish a reliable scale-up procedure in order to successfully design and construct industrial scale SBC reactors. As pointed out before, in order to design a bubble column reactor, the volumetric mass transfer coefficient needs to be known within an acceptable range of error. Many correlations have been forward so far to estimate the mass transfer rate in bubble column reactors. Nevertheless, it should be highlighted that most of the proposed correlations in the literature are based on the results which were obtained from laboratory scale reactors. Another shortcoming of most existing correlations is that the indirect measurement techniques were employed to determine the $k_L a$. Considering the abovementioned drawbacks of previous models, in the present research, the dissolved oxygen probe was utilized to measure $k_L a$ in a pilot scale slurry bubble column. Consequently, we believe that the reported results and developed correlations can be certainly relevant to the design and performance of large-scale industrial SBCRs.

4.5.1 Dimensionless analysis to derive correlation

In order to develop correlations for predicting $k_L a$ in both two-phase and three-phase systems, the first step is dimensionless analysis. The Buckingham's π theorem is applied to define the independent dimensionless groups which have effects on the volumetric mass transfer coefficient. According to our experiments, generally, there are eight physical variables ($n = 8$) that affect the mass transfer for air-water and air-water-glass beads systems.

Operating conditions, design variables and the properties of phases (e.g. liquid phase density) are the effective parameters. Given this, it is assumed that:

$$k_L a = f(U_G, g, D_C, \rho_L, \rho_G, \mu_L, D_L, \sigma_L) \quad (4-2)$$

These variables contain three physical dimensions ($m = 3$): mass $[M]$, length $[L]$, and time $[T]$. Therefore, the number of dimensionless numbers are, $\pi' = (n - m) = 8 - 3 = 5$ [116].

The dimensionless numbers are as follows,

Table 4.2- Dimensionless numbers used in this work

| Dimensionless number | | Concept |
|---|----------------|---|
| $\pi_1 = \frac{\mu_L}{\rho_L D_L}$ | Schmidt number | $Sc = \frac{\text{Viscous Diffusion Rate}}{\text{Mass Diffusion Rate}}$ |
| $\pi_2 = \frac{g \rho_L^2 D_C^3}{\mu_L^2}$ | Galilei number | $Ga = \frac{\text{Gravitational Force}}{\text{Viscous Forces}}$ |
| $\pi_3 = \frac{U_G}{\sqrt{D_C g}}$ | Froude number | $Fr = \frac{\text{Flow Inertia Force}}{\text{Gravitational Force}}$ |
| $\pi_4 = \frac{g(\rho_L - \rho_G) D_C^2}{\sigma_L}$ | Bond number | $Bo = \frac{\text{Buoyancy Force}}{\text{Surface Tension Force}}$ |
| $\pi_5 = \frac{\rho_G}{\rho_L}$ | - | The ratio of gas density to the liquid density |

The volumetric mass transfer coefficient for 2-phase and 3-phase systems can be calculated by the following equation by utilizing the dimensionless numbers,

$$Sh = f\left(Sc, Ga, Fr, Bo, \frac{\rho_G}{\rho_L}\right) \quad (4-3)$$

Where Sh is the Sherwood number ($Sh = \frac{k_L a \times D_C^2}{D_L}$)

The following correlation is proposed based on the mentioned dimensionless numbers and by rearranging equation 4-3,

$$k_L a = a_1 Sc^{a_2} Ga^{a_3} Fr^{a_4} Bo^{a_5} \left(\frac{\rho_G}{\rho_L}\right)^{a_6} \left(\frac{D_L}{D_C^2}\right) \quad (4-4)$$

Genetic Algorithm function (GA) in MATLAB was applied to determine a_i values ($1 \leq i \leq 6$) of equation 4-4 by using 105 data points obtained for two and three phase systems experiments.

The correlation for the two-phase air-water system and a three-phase air-water-glass beads system is:

$$k_L a = 0.06 Sc^{0.85} Ga^{0.47} Fr^{0.11} Bo^{0.14} \left(\frac{\rho_G}{\rho_L} \right)^{0.22} \left(\frac{D_L}{D_C^2} \right) \quad (4-5)$$

This correlation is valid for the following ranges,

$$392.4 \leq Sc \leq 501.4$$

$$1.86 \times 10^{11} \leq Ga \leq 2.42 \times 10^{11}$$

$$3.31 \times 10^{-3} \leq Fr \leq 1.31 \times 10^{-1}$$

$$1.14 \times 10^4 \leq Bo \leq 1.23 \times 10^4$$

$$1.14 \times 10^{-3} \leq \frac{\rho_g}{\rho_l} \leq 1.22 \times 10^{-3}$$

The MAPE, standard error (SE) of the fitting are 4.8%, $\pm 0.27\%$ respectively.

It should be mentioned that the physical properties of the slurry phase will be used in equation 4-5. The density, viscosity, and diffusivity of the slurry phase can be calculated based on the formulas provided in table 4-3. It should be noted that the presence of solid particles does not influence the liquid surface tension.

Table 4.3- Formulas for calculating density, viscosity, and diffusivity of the slurry phase

| | |
|--|--|
| Slurry phase density (kg/m^3): | $\rho_{SL} = \rho_L(1 - C_V) + \rho_S C_V$ ([117]) |
| Slurry phase viscosity ($Pa \cdot s$): | $\mu_{SL} = \mu_L(1 + 4.5 C_V)$ [27] |
| Slurry phase diffusivity (m^2/s): | $D_{SL} = 5 \times 10^{-11} \mu_{SL}^{-0.57}$ [59] |

Figure 4-7 compares the values predicted by the developed model (Equation 4-5) with those obtained from the experimental data at different solid concentrations ($0 \leq C_V \leq 5\%$) and particle sizes (71 and 156 μm). In this figure, the center solid line represents 100% accordance between

the model and experimental data, while the dashed lines show $\pm 4.8\%$ *MAPE*. Considering Figure 4-7, it is evident that the developed correlation can reproduce the experimental results for the volumetric mass transfer coefficient with high accuracy. Mean absolute percentage errors of all points fall below 4.81% and the standard deviation is approximately 0.27 %, indicating a good agreement between model and experimental data.

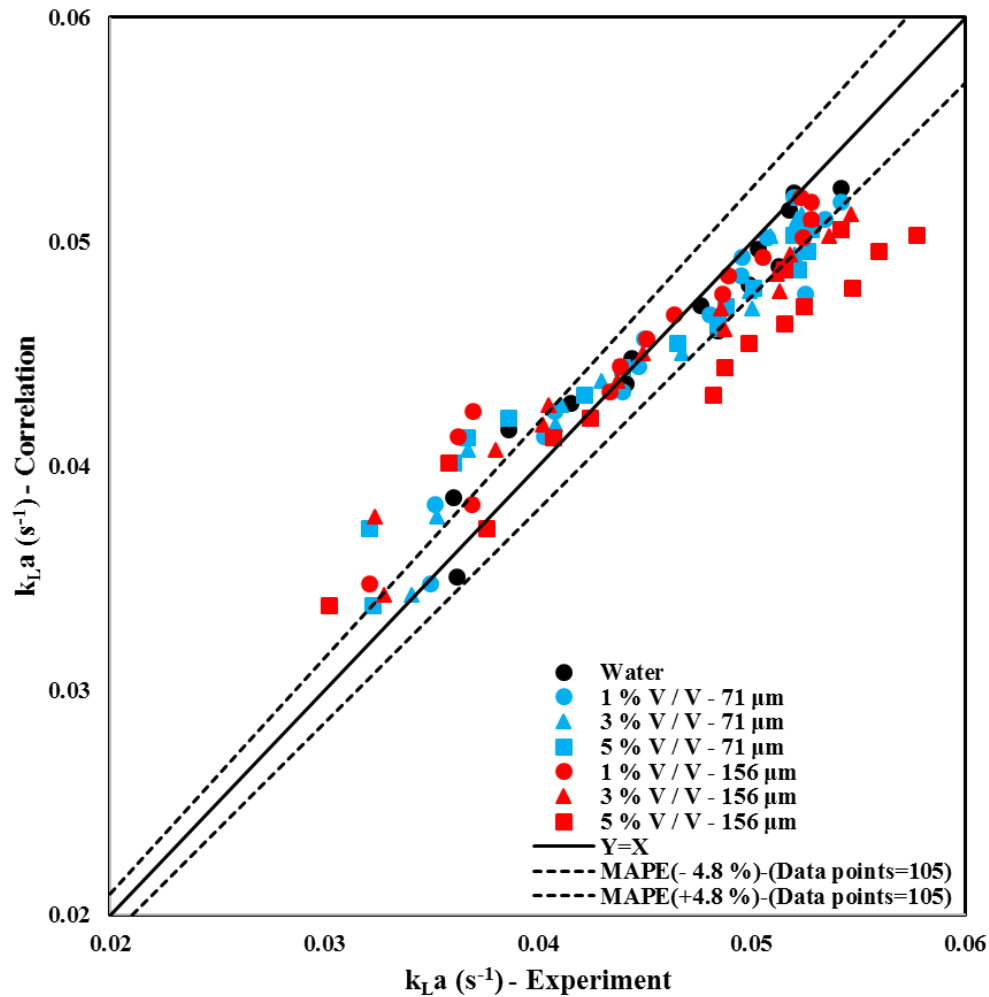


Figure 4.7- Comparison between the experimental and the predicted value of k_La

4.5.2 Applying developed correlation to previous experimental results

Five different data sets from the literature were selected in order to verify the proposed correlation for slurry bubble column reactors. Table 4-4 summarizes the process conditions and the design parameters of the bubble column at which the experiments were conducted.

Our proposed correlation was utilized to predict the $k_L a$ of these works based on the reported physical properties and process situations. A comparison between the predicted values and the experimental results is shown in Figure 4-8. Mean absolute percentage error of all points is 23.43% and the standard deviation is 2.82%, which show a fairly good agreement between predicted values and the experimental data. It should be mentioned that some of these errors can be attributed to the difference of the design parameters (such as the gas distributors) which were not included in the developed correlation.

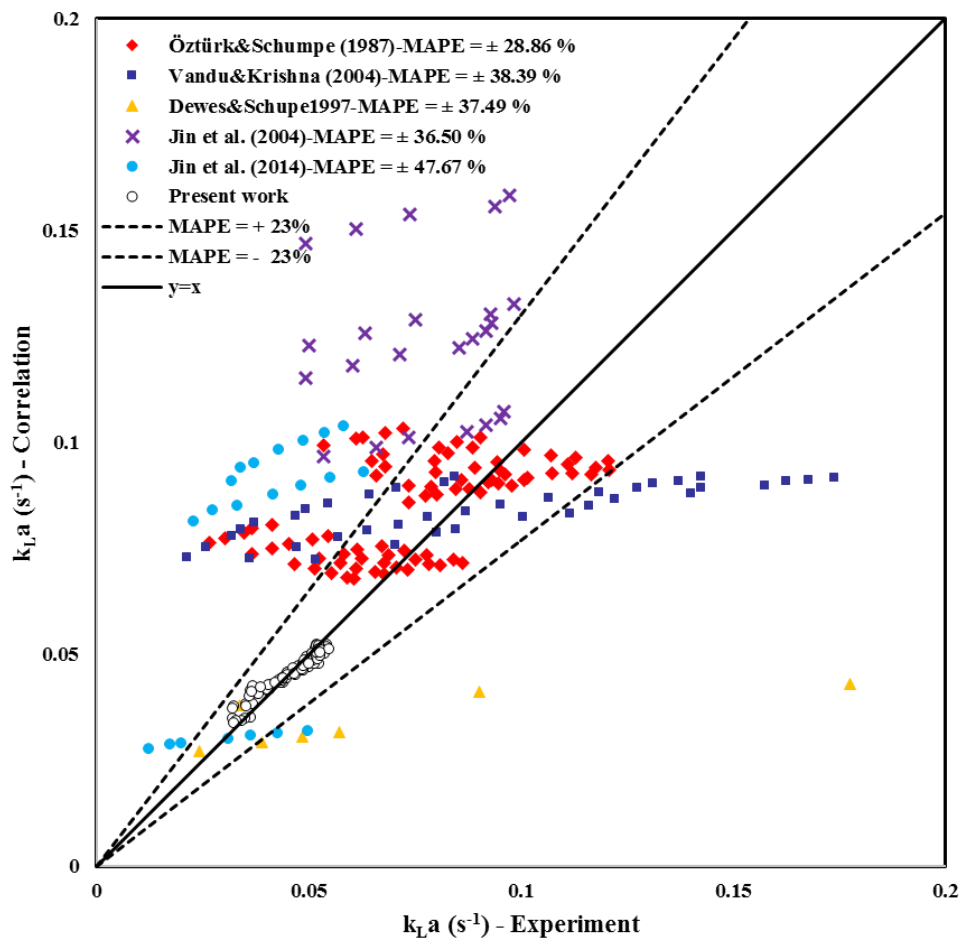


Figure 4.8- Applying developed a correlation of $k_L a$ to previous experimental works

Table 4.4- Literature list for the SBCs parametric study

| | |
|---|---|
| Jin et al. (2004) [118] | |
| <i>Gas</i> | Air: $U_G = (3 - 10) \text{ cm/s}$ |
| <i>Liquid</i> | Water |
| <i>Solid</i> | Quartz Sand $C_V = (0 - 20)\%$ |
| <i>Column dimension</i> | $H_C = (40 - 60) \text{ cm}$, $D_C = (6 - 10) \text{ cm}$ |
| <i>Gas sparger</i> | 4 Nozzles ($d_0=8 \text{ mm}$) |
| Vandu et al. (2004) [10] | |
| <i>Gas</i> | Air: $U_G = (0 - 40) \text{ cm/s}$ |
| <i>Liquid</i> | Paraffin Oil |
| <i>Solid</i> | Alumina based Catalyst: $C_V = (0 - 25)\%$ |
| <i>Column dimension</i> | $H_C = (134 - 136) \text{ cm}$, $D_C = (10) \text{ cm}$ |
| <i>Gas sparger</i> | Perforated plate ($d_0=0.5 \text{ mm}$, 199 holes) |
| Öztürk & Schumpe (1987) [11] | |
| <i>Gas</i> | Air: $U_G = (0 - 8) \text{ cm/s}$ |
| <i>Liquid</i> | Water, Ligroin, Tetralin, Aq: Na_2SO_4 (0.8 M)) |
| <i>Solid</i> | PE (24.6, 106 μm), PVC (82 μm), AC (5.4 μm), Kieselguhr (6.6 μm), Al_2O_3 (10.5 μm), $C_V = (0 - 12)\%$ |
| <i>Column dimension</i> | $H_C = (85) \text{ cm}$, $D_C = (9.5) \text{ cm}$ |
| <i>Gas sparger</i> | 2 Single orifice tubes, ($d_0=3, 0.9 \text{ mm}$) |
| Jin et al. (2014) [119] | |
| <i>Gas</i> | H_2 , CO, CO_2 , $U_G = (3 - 10) \text{ cm/s}$ |
| <i>Liquid</i> | Paraffin |
| <i>Solid</i> | Quartz Sand, (150-200 μm), $C_V = (0 - 20)\%$ |
| <i>Column dimension</i> | $H_C = (40 - 60) \text{ cm}$, $D_C = (10) \text{ cm}$ |
| <i>Gas sparger</i> | Perforated Plate, ($d_0= 8 \text{ mm}$) |
| Dewes & Schumpe (1997) [120] | |
| <i>Gas</i> | Air, He, N_2 , SF_6 , $U_G = (1 - 8) \text{ cm/s}$ |
| <i>Liquid</i> | Water, Sodium sulfate (0.8 M) |
| <i>Solid</i> | Xanthan gum, kieselguhr (22 μm), Alumina (7 μm) , $C_V = (0 - 18)\%$ |
| <i>Column dimension</i> | $H_C = (137) \text{ cm}$, $D_C = (11.5) \text{ cm}$ |
| <i>Gas sparger</i> | Perforated Plate, ($d_0=1 \text{ mm}$, 7 holes) |

4.5.3 Comparison of the present correlation with other correlations

Some of the existing correlations for SBCRs available in the literature (Table 4-5) were selected and compared in terms of prediction accuracy to our developed model.

Table 4.5- Dimensionless correlations for prediction of $k_L a$ in BCs in some literature

| Authors | Correlation Proposed |
|---------------------------------|--|
| Hikita et al. (1981)[86] | $k_L a = 14.9 g^{0.752} U_G^{0.76} \rho_L^{0.852} \mu_G^{0.243} \mu_L^{-0.079} \sigma^{-1.016} D_A^{0.604}$ |
| Shah et al. (1982)[24] | $k_L a = 0.467 u_G^{0.82}$ |
| Fukuma et al. (1987)[121] | $k_L a = 4.5 \times 10^{-4} (Sc)^{0.5} (Bo)^{-0.2} (Ga)^{0.8} (6\varepsilon_G) \frac{D_A}{d_{vs}^2}$ |
| Öztürk et al. (1987)[59] | $k_L a = 0.62 (Sc)^{0.5} (Bo)^{0.33} (Ga)^{0.29} (Fr)^{0.68} \left(\frac{\rho_G}{\rho_L} \right)^{0.04} \frac{D_A}{d_B^2}$ |
| Jordan & Schumpe (2001)[122] | $k_L a = 0.522 (Sc)^{0.5} (Bo)^{0.34} (Ga)^{0.27} (Fr)^{0.72} \left(1 + 1.32 Fr^{0.37} \left(\frac{\rho_G}{\rho_L} \right)^{0.49} \right) \frac{D_A}{d_B^2}$ |
| Behkish et al. (2002)[103] | $k_L a = 0.18 (Sc)^{-0.6} \left(\frac{\rho_{SL} v_A}{M_B} \right)^{-2.84} (\rho_G u_G)^{0.49} e^{-2.66 C_V}$ |
| Jin et al. (2004)[118] | $k_L a = C \left(1 - \frac{C_V}{0.7} \right)^{0.802} \mu_{SL}^{-0.244} u_G^{0.721} \rho_S^{0.143}$ |
| Jin et al. (2014)[119] | $k_L a = 3.051 \left(\frac{\rho_{SL} v_A}{M_B} \right)^{-1.193} (Sc)^{-0.734} (\rho_G u_G)^{0.524} \left(1 - \frac{C_V}{0.85} \right)^{2.303}$ |

The listed equations in Table 4-5 were employed to estimate the volumetric mass transfer coefficient based on the physical properties and process parameters. A comparison between the predicted values and the experimental results is shown in Figure 4-9. Mean absolute percentage error of all points is 17.65%. As shown before, the MAPE for the correlation proposed in this study is 4.81%, which is by far smaller than that for the correlation reported in previous works.

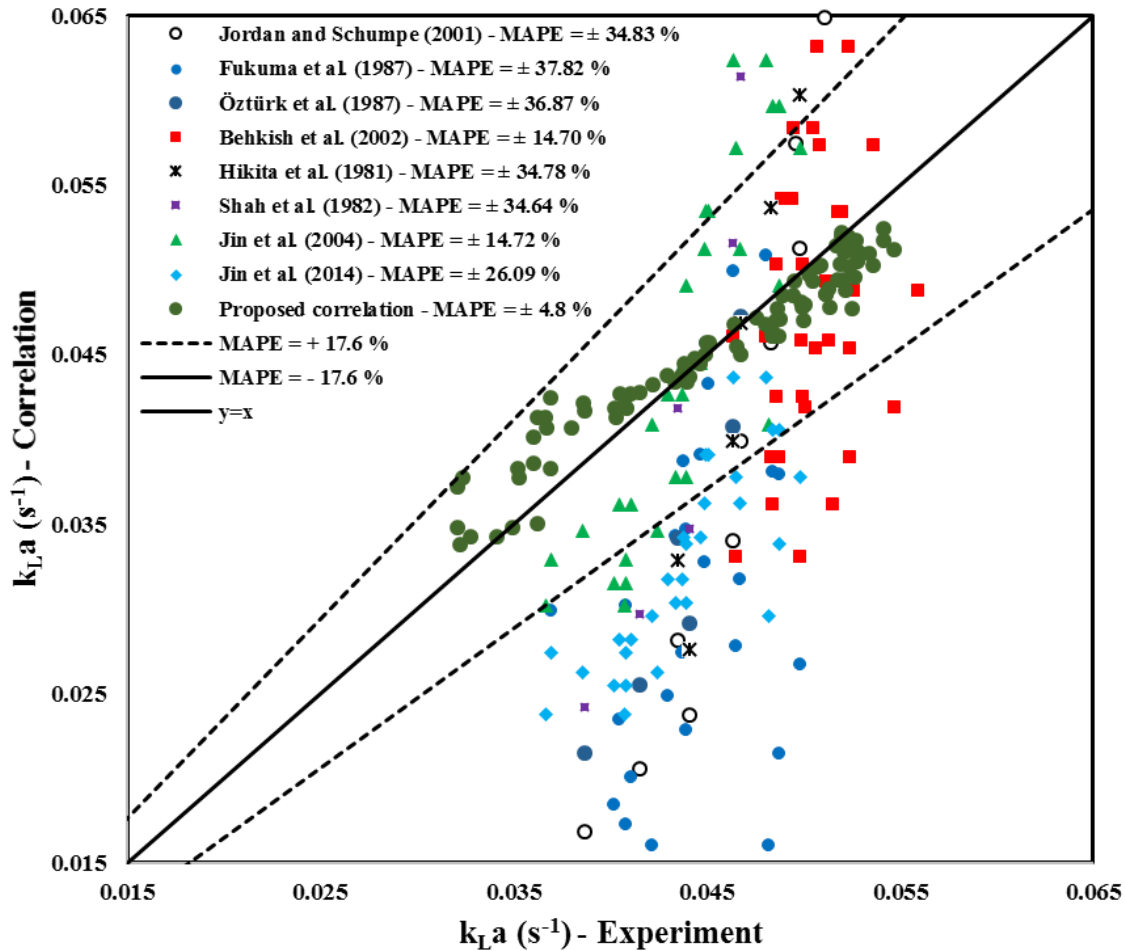


Figure 4.9- Comparison between some proposed correlations for predicting $k_L a$

CHAPTER 5 CONCLUSION AND RECOMMANDATIONS

5.1 Conclusion

In this study, we achieved a better understanding of the effect of solid concentration, particle size and the superficial gas velocity on the volumetric mass transfer coefficient in the slurry bubble column. Highlighted conclusions of the present work are indicated below.

- 1- In both Homogeneous and Heterogenous flow regimes in air-water system, the variations of the mass transfer coefficient in the radial direction are not considerable and we can assume a uniform radial distribution for $k_L a$.
- 2- In low gas velocities, it is observed that the presence of solids particles negatively affects the mass transfer, while, on the contrary, at high velocities, solids particles lead to increase in the volumetric mass transfer coefficient.
- 3- Using the larger size glass beads lead to considerable enhancement in the mass transfer coefficient in comparison to the small particles mainly due to turbulence increasing in the gas-liquid interface by the particles.
- 4- The predicted values by the developed correlation show a fairly good agreement with the experimental data of the present work and the literature experimental data.

5.2 Recommendations

Successful design and operation of the slurry bubble column reactor completely depend on the knowledge that we have about the effect of the various parameters on the hydrodynamic, mass transfer, heat transfer and the kinetics. In the present study, the effects of the solid concentration and the particle size on $k_L a$ were investigated. Based on the literature review, there are lots of unknown phenomena that can be the subject of future studies. The author can suggest the following points in order to continue this study and to obtain a better understanding of the effect of various parameters on the volumetric mass transfer coefficient. The recommendations are as follows:

- 1- Majority of the applications in the slurry bubble columns are in the high pressure and high temperature. So, it can be useful to study the effect of the pressure and temperature on the volumetric mass transfer coefficient.
- 2- In the present study, a hydrophilic solid particle was used for the experiments. These particles result in a reduction in the gas holdup and consequently $k_L a$. Study the effect of the degree of hydrophobicity on the volumetric mass transfer coefficient may provide a better understanding of the system
- 3- It is very important to know the effect of the parameters on the k_L rather than $k_L a$. Therefore, it will be interesting to measure the interfacial surface area in addition to the $k_L a$ to estimate the k_L . It is possible to use optical fiber probes to measure the local bubble size distribution and to calculate the interfacial surface area.
- 4- In industrial reactors, various kind of internals are used inside the slurry bubble column. These internals affect the hydrodynamic and lead to change in the volumetric mass transfer coefficient. For future studies, the effect of the internals on the local $k_L a$ can be investigated.

REFERENCES

- [1] G. Vázquez, M. A. Cancela, C. Riverol, E. Alvarez, and J. M. Navaza, "Application of the Danckwerts method in a bubble column: Effects of surfactants on mass transfer coefficient and interfacial area," *Chemical Engineering Journal*, vol. 78, no. 1, pp. 13-19, 2000/07/01/ 2000.
- [2] T. Miyahara, H. Hamanaka, T. Takino, Y. Akagi, and K. Okada, "Gas Holdup, Gas-Liquid Interfacial Area and Mass Transfer Coefficient in External-loop Airlift Bubble Column Containing Low Density Particles," *JOURNAL OF CHEMICAL ENGINEERING OF JAPAN*, vol. 30, no. 5, pp. 958-961, 1997.
- [3] K. Akita and F. Yoshida, "Bubble Size, Interfacial Area, and Liquid-Phase Mass Transfer Coefficient in Bubble Columns," *Industrial & Engineering Chemistry Process Design and Development*, vol. 13, no. 1, pp. 84-91, 1974/01/01 1974.
- [4] A. H. P. Skelland, *Diffusional mass transfer* [by] A. H. P. Skelland (no. Accessed from <http://nla.gov.au/nla.cat-vn353232>). New York: Wiley, 1974.
- [5] R. E. Treybal, *Mass-transfer operations*: Robert E. Treybal, 3rd -- ed. (no. Book, Whole). New York: McGraw-Hill, 1980.
- [6] L. S. Omar M. Basha, Ahmed Abdel-Wahab and Badie I. Morsi*, "Fischer–Tropsch Synthesis in Slurry Bubble Column Reactors: Experimental Investigations and Modeling – A Review," *Int. J. Chem. React. Eng*, vol. 3, no. 13, pp. 201–288, 2015.
- [7] N. Kantarci, F. Borak, and K. O. Ulgen, "Bubble column reactors," *Process Biochemistry*, vol. 40, no. 7, pp. 2263-2283, 6// 2005.
- [8] S. Nedeltchev, "Theoretical prediction of mass transfer coefficients in both gas–liquid, and slurry bubble columns," *Chemical Engineering Science*, vol. 157, pp. 169-181, 1/10/ 2017.
- [9] A. Behkish, R. Lemoine, L. Sehabiague, R. Oukaci, and B. I. Morsi, "Gas holdup and bubble size behavior in a large-scale slurry bubble column reactor operating with an organic liquid under elevated pressures and temperatures," *Chemical Engineering Journal*, vol. 128, no. 2–3, pp. 69-84, 4/1/ 2007.

- [10] C. O. Vandu and R. Krishna, "Volumetric mass transfer coefficients in slurry bubble columns operating in the churn-turbulent flow regime," *Chemical Engineering and Processing: Process Intensification*, vol. 43, no. 8, pp. 987-995, 8// 2004.
- [11] S. S. Öztürk and A. Schumpe, "The influence of suspended solids on oxygen transfer to organic liquids in a bubble column," *Chemical Engineering Science*, vol. 42, no. 7, pp. 1781-1785, 1987/01/01/ 1987.
- [12] O. Ozkan, A. Calimli, R. Berber, and H. Oguz, "Effect of inert solid particles at low concentrations on gas–liquid mass transfer in mechanically agitated reactors," *Chemical Engineering Science*, vol. 55, no. 14, pp. 2737-2740, 2000/04/07/ 2000.
- [13] P. Mena, A. Ferreira, J. A. Teixeira, and F. Rocha, "Effect of some solid properties on gas–liquid mass transfer in a bubble column," *Chemical Engineering and Processing: Process Intensification*, vol. 50, no. 2, pp. 181-188, 2011/02/01/ 2011.
- [14] S. P. Godbole, A. Schumpe, and Y. T. Shah, "HYDRODYNAMICS AND MASS TRANSFER IN BUBBLE COLUMNS: EFFECT OF SOLIDS," *Chemical Engineering Communications*, vol. 24, no. 4-6, pp. 235-258, 1983/12/01 1983.
- [15] E. L. Paul, V. A. Atiemo-Obeng, and S. M. Kresta, *Handbook of industrial mixing: science and practice*. John Wiley & Sons, 2004.
- [16] H. S. Fogler, *Elements of chemical reaction engineering*, 4th -- ed. Upper Saddle River, N.J: Prentice Hall Professional Technical Reference, 2006.
- [17] P. C. Mena, F. A. Rocha, J. A. Teixeira, P. Sechet, and A. Cartellier, "Measurement of gas phase characteristics using a monofibre optical probe in a three-phase flow," *Chemical Engineering Science*, vol. 63, no. 16, pp. 4100-4115, 2008/08/01/ 2008.
- [18] M. C. Gruber, S. Radl, and J. G. Khinast, "Effect of bubble–particle interaction models on flow predictions in three-phase bubble columns," *Chemical Engineering Science*, vol. 146, pp. 226-243, 2016.
- [19] Y. D. Li, S. M. Lu, and Q. P. Guan, "A Review of Theoretical Research on Partial Parameters in Three-Phase Slurry Bubble Column Reactor," in *Advanced Materials Research*, 2014, vol. 838, pp. 2404-2412: Trans Tech Publ.

- [20] S. Degaleesan, M. Dudukovic, and Y. Pan, "Experimental study of gas-induced liquid-flow structures in bubble columns," *AIChE Journal*, vol. 47, no. 9, pp. 1913-1931, 2001.
- [21] L. Sehabiague et al., "Assessing the performance of an industrial SBCR for Fischer–Tropsch synthesis: Experimental and modeling," *AIChE Journal*, vol. 61, no. 11, pp. 3838-3857, 2015.
- [22] M. M. Carbonell and R. J. C. e. s. Guirardello, "Modelling of a slurry bubble column reactor applied to the hydroconversion of heavy oils," vol. 52, no. 21-22, pp. 4179-4185, 1997.
- [23] G. Besagni and F. Inzoli, "The effect of electrolyte concentration on counter-current gas–liquid bubble column fluid dynamics: Gas holdup, flow regime transition, and bubble size distributions," *Chemical Engineering Research and Design*, vol. 118, pp. 170-193, 2// 2017.
- [24] Y. T. Shah, B. G. Kelkar, S. P. Godbole, and W.-D. Deckwer, "Design parameters estimations for bubble column reactors," *AIChE Journal*, vol. 28, no. 3, pp. 353-379, 1982.
- [25] P. Chen, "Modeling the fluid dynamics of bubble column flows," 3140691 D.Sc., Washington University in St. Louis, Ann Arbor, 2004.
- [26] W.-D. Deckwer, Y. Louisi, A. Zaidi, and M. Ralek, "Hydrodynamic Properties of the Fischer-Tropsch Slurry Process," *Industrial & Engineering Chemistry Process Design and Development*, vol. 19, no. 4, pp. 699-708, 1980/10/01 1980.
- [27] S. C. Saxena and Z. D. Chen, "HYDRODYNAMICS AND HEAT TRANSFER OF BAFFLED AND UNBAFFLED SLURRY BUBBLE COLUMNS," in *Reviews in Chemical Engineering* vol. 10, ed, 1994, p. 193.
- [28] C. Guy, P. J. Carreau, and J. Paris, "Mixing characteristics and gas hold-up of a bubble column," *The Canadian Journal of Chemical Engineering*, vol. 64, no. 1, pp. 23-35, 1986.
- [29] N. Deen, Mudde, R., Kuipers, J., Zehner, P. and Kraume, M, "Bubble Columns," 2000.
- [30] R. Krishna and J. M. van Baten, "Mass transfer in bubble columns," *Catalysis Today*, vol. 79–80, pp. 67-75, 4/30/ 2003.

- [31] C. L. Hyndman, F. Larachi, and C. Guy, "Understanding gas-phase hydrodynamics in bubble columns: a convective model based on kinetic theory," *Chemical Engineering Science*, vol. 52, no. 1, pp. 63-77, 1997/01/01/ 1997.
- [32] B. N. Thorat and J. B. Joshi, "Regime transition in bubble columns: experimental and predictions," *Experimental Thermal and Fluid Science*, vol. 28, no. 5, pp. 423-430, 4// 2004.
- [33] A. Behkish, "Hydrodynamic and mass transfer parameters in large-scale slurry bubble column reactors," University of Pittsburgh, 2005.
- [34] C. Leonard, J. H. Ferrasse, O. Boutin, S. Lefevre, and A. Viand, "Bubble column reactors for high pressures and high temperatures operation," *Chemical Engineering Research and Design*, vol. 100, pp. 391-421, 2015/08/01/ 2015.
- [35] A. Sarrafi, H. Müller-Steinhagen, J. M. Smith, and M. Jamialahmadi, *Gas Hold-up in Homogeneous and Heterogeneous Gas-Liquid Bubble Column Reactors*. 1999, pp. 11-21.
- [36] J. B. Joshi, N. S. Deshpande, M. Dinkar, and D. V. Phanikumar, "Hydrodynamic stability of multiphase reactors," in *Advances in Chemical Engineering*, vol. 26: Academic Press, 2001, pp. 1-130.
- [37] R. Krishna, P. M. Wilkinson, and L. L. Van Dierendonck, "A model for gas holdup in bubble columns incorporating the influence of gas density on flow regime transitions," *Chemical Engineering Science*, vol. 46, no. 10, pp. 2491-2496, 1991/01/01/ 1991.
- [38] F. YAMASHITA and H. INOUE, "Gas holdup in bubble columns," *Journal of Chemical Engineering of Japan*, vol. 8, no. 4, pp. 334-336, 1975.
- [39] H. F. Bach and T. Pilhofer, *Variation of Gas Holdup in Bubble Columns With Physical Properties of Liquids and Operating Parameters of Columns*. 1978, pp. 270-275.
- [40] F. Kašánek, M. Rylek, and J. Nývlt, "Scaling-up of bubble-type reactors and the effect of reactor size on gas holdup in water-air systems," *Collection of Czechoslovak Chemical Communications*, vol. 39, no. 11, pp. 3246-3255, 1974.

- [41] H. Li and A. Prakash, "Influence of slurry concentrations on bubble population and their rise velocities in a three-phase slurry bubble column," *Powder Technology*, vol. 113, no. 1–2, pp. 158-167, 11/20/ 2000.
- [42] Y. T. Shah, *Gas liquid solid reactor design*. McGraw-Hill International Book Company, 1979.
- [43] Y. Wu, B. Cheng Ong, and M. H. Al-Dahhan, "Predictions of radial gas holdup profiles in bubble column reactors," *Chemical Engineering Science*, vol. 56, no. 3, pp. 1207-1210, 2// 2001.
- [44] P. C. Mena, M. C. Ruzicka, F. A. Rocha, J. A. Teixeira, and J. Drahoš, "Effect of solids on homogeneous–heterogeneous flow regime transition in bubble columns," *Chemical Engineering Science*, vol. 60, no. 22, pp. 6013-6026, 2005/11/01/ 2005.
- [45] H. Hikita, S. Asai, K. Tanigawa, K. Segawa, and M. Kitao, "Gas hold-up in bubble columns," *The Chemical Engineering Journal*, vol. 20, no. 1, pp. 59-67, 1980/01/01/ 1980.
- [46] D. N. Miller, "Gas Holdup and Pressure Drop in Bubble Column Reactors," *Industrial & Engineering Chemistry Process Design and Development*, vol. 19, no. 3, pp. 371-377, 1980/07/01 1980.
- [47] L.-S. Fan, A. Matsuura, and S.-H. Chern, "Hydrodynamic characteristics of a gas-liquid-solid fluidized bed containing a binary mixture of particles," *AIChE Journal*, vol. 31, no. 11, pp. 1801-1810, 1985.
- [48] I. G. Reilly, D. S. Scott, T. De Bruijn, A. Jain, and J. Piskorz, "A correlation for gas holdup in turbulent coalescing bubble columns," *The Canadian Journal of Chemical Engineering*, vol. 64, no. 5, pp. 705-717, 1986.
- [49] A. Prakash, A. Margaritis, H. Li, and M. A. Bergougnou, "Hydrodynamics and local heat transfer measurements in a bubble column with suspension of yeast," *Biochemical Engineering Journal*, vol. 9, no. 2, pp. 155-163, 12// 2001.
- [50] R. Krishna, J. W. A. D. Swart, J. Ellenberger, G. B. Martina, and C. Maretto, "Gas holdup in slurry bubble columns: Effect of column diameter and slurry concentrations," *AIChE Journal*, vol. 43, no. 2, pp. 311-316, 1997.

- [51] A. Schumpe and G. Grund, "The gas disengagement technique for studying gas holdup structure in bubble columns," *The Canadian Journal of Chemical Engineering*, vol. 64, no. 6, pp. 891-896, 1986.
- [52] L. Z. Pino, R. B. Solari, S. Siquier, L. Antonio Estévez, M. M. YÉpez, and A. E. SÁez, "EFFECT OF OPERATING CONDITIONS ON GAS HOLDUP IN SLURRY BUBBLE COLUMNS WITH A FOAMING LIQUID," *Chemical Engineering Communications*, vol. 117, no. 1, pp. 367-382, 1992/09/01 1992.
- [53] S. C. Saxena, N. S. Rao, and A. C. Saxena, "HEAT-TRANSFER AND GAS-HOLDUP STUDIES IN A BUBBLE COLUMN: AIR-WATER-GLASS BEAD SYSTEM," *Chemical Engineering Communications*, vol. 96, no. 1, pp. 31-55, 1990/10/01 1990.
- [54] J. G. Daly, S. A. Patel, and D. B. Bukur, "Measurement of gas holdups and sauter mean bubble diameters in bubble column reactors by dynamics gas disengagement method," *Chemical Engineering Science*, vol. 47, no. 13, pp. 3647-3654, 1992/09/01/ 1992.
- [55] K. Koide, A. Takazawa, M. Komura, and H. MATSUNAGA, "Gas holdup and volumetric liquid-phase mass transfer coefficient in solid-suspended bubble columns," *Journal of chemical engineering of Japan*, vol. 17, no. 5, pp. 459-466, 1984.
- [56] M. Lockett and R. D. Kirkpatrick, *Ideal bubbly flow and actual flow on bubble columns*. 1975, pp. 267-273.
- [57] H. L. a. A. Prakash, "Heat Transfer and Hydrodynamics in a Three-Phase Slurry Bubble Column," *Ind. Eng. Chem. Res.*, vol. 36, pp. 4688-4694, 1997.
- [58] L. S. Fan, G. Q. Yang, D. J. Lee, K. Tsuchiya, and X. Luo, "Some aspects of high-pressure phenomena of bubbles in liquids and liquid–solid suspensions," *Chemical Engineering Science*, vol. 54, no. 21, pp. 4681-4709, 1999/11/01/ 1999.
- [59] S. S. öztürk, A. Schumpe, and W. D. Deckwer, "Organic liquids in a bubble column: Holdups and mass transfer coefficients," *AIChE Journal*, vol. 33, no. 9, pp. 1473-1480, 1987.
- [60] C. Tang and T. J. Heindel, "Time-dependent gas holdup variation in an air–water bubble column," *Chemical Engineering Science*, vol. 59, no. 3, pp. 623-632, 2004/02/01/ 2004.

- [61] V. P. Chilekar, J. van der Schaaf, B. F. M. Kuster, J. T. Tinge, and J. C. Schouten, "Influence of elevated pressure and particle lyophobicity on hydrodynamics and gas–liquid mass transfer in slurry bubble columns," *AIChE Journal*, vol. 56, no. 3, pp. 584-596, 2010.
- [62] N.-S. Cheng and A. W.-K. Law, "Exponential formula for computing effective viscosity," *Powder Technology*, vol. 129, no. 1, pp. 156-160, 2003/01/08/ 2003.
- [63] K. Tsuchiya, A. Furumoto, L.-S. Fan, and J. Zhang, "Suspension viscosity and bubble rise velocity in liquid-solid fluidized beds," *Chemical Engineering Science*, vol. 52, no. 18, pp. 3053-3066, 1997/09/01/ 1997.
- [64] F. Liang-Shih and K. Tsuchiya, *Bubble wake dynamics in liquids and liquid-solid suspensions*. Butterworth-Heinemann, 2013.
- [65] A. Ferreira, C. Ferreira, J. A. Teixeira, and F. Rocha, "Temperature and solid properties effects on gas–liquid mass transfer," *Chemical Engineering Journal*, vol. 162, no. 2, pp. 743-752, 2010/08/15/ 2010.
- [66] Y. Kato, A. Nishiwaki, T. Kago, T. Fukuda, and S. Tanaka, "Gas Holdup and Overall Volumetric Absorption Coefficient in Bubble Columns with Suspended Solid Particles
Absorption rate of oxygen by aqueous sodium sulfite solution," *Chemical engineering*, vol. 36, no. 12, pp. 1333-1337, a1, 1972.
- [67] B. G. K. Swap Kara, and Yatish T. Shah, "Hydrodynamics and axial mixing in a three-phase bubble column," *Ind Eng Chem Process Des Dev*, vol. 21, pp. 584–594, 1982.
- [68] S. K. Eizo Sada, Hidehumi Yoshii, Toshihiko Yamanishi, Akio Nakanishi, "Performance of the gas bubble column in molten salt systems," *Ind. Eng. Chem. Process Des. Dev.*, vol. 23, pp. 151–154, 1984.
- [69] J. W. A. De Swart, R. E. van Vliet, and R. Krishna, "Size, structure and dynamics of “large” bubbles in a two-dimensional slurry bubble column," *Chemical Engineering Science*, vol. 51, no. 20, pp. 4619-4629, 1996/10/01/ 1996.

- [70] R. Pohorecki, W. Moniuk, and A. Zdrójkowski, "Hydrodynamics of a bubble column under elevated pressure," *Chemical Engineering Science*, vol. 54, no. 21, pp. 5187-5193, 1999/11/01/ 1999.
- [71] Y. T. Shah, S. Joseph, D. N. Smith, and J. A. Ruether, "Two-bubble class model for churn turbulent bubble-column reactor," *Industrial & Engineering Chemistry Process Design and Development*, vol. 24, no. 4, pp. 1096-1104, 1985/10/01 1985.
- [72] M. Fukuma, K. Muroyama, and A. Yasunishi, "PROPERTIES OF BUBBLE SWARM IN A SLURRY BUBBLE COLUMN," *Journal of Chemical Engineering of Japan*, vol. 20, no. 1, pp. 28-33, 1987.
- [73] R. Schäfer, C. Merten, and G. Eigenberger, "Bubble size distributions in a bubble column reactor under industrial conditions," *Experimental Thermal and Fluid Science*, vol. 26, no. 6-7, pp. 595-604, 8// 2002.
- [74] X. Luo, D. J. Lee, R. Lau, G. Yang, and L.-S. Fan, "Maximum stable bubble size and gas holdup in high-pressure slurry bubble columns," *AIChE Journal*, vol. 45, no. 4, pp. 665-680, 1999.
- [75] M. J. Prince and H. W. Blanch, "Bubble coalescence and break-up in air-sparged bubble columns," *AIChE Journal*, vol. 36, no. 10, pp. 1485-1499, 1990.
- [76] P. M. Wilkinson and L. L. v. Dierendonck, "Pressure and gas density effects on bubble break-up and gas hold-up in bubble columns," *Chemical Engineering Science*, vol. 45, no. 8, pp. 2309-2315, 1990/01/01/ 1990.
- [77] I. Taylor Geoffrey, "The instability of liquid surfaces when accelerated in a direction perpendicular to their planes. I," *Proceedings of the Royal Society of London. Series A. Mathematical and Physical Sciences*, vol. 201, no. 1065, pp. 192-196, 1950/03/22 1950.
- [78] R. Bellman and R. H. Pennington, "Effects of surface tension and viscosity on Taylor instability," *Quarterly of Applied Mathematics*, vol. 12, no. 2, pp. 151-162, 1954.
- [79] T.-J. Lin, K. Tsuchiya, and L.-S. Fan, "Bubble flow characteristics in bubble columns at elevated pressure and temperature," *AIChE Journal*, vol. 44, no. 3, pp. 545-560, 1998.

- [80] J. F. Walter and H. W. Blanch, "Bubble break-up in gas—liquid bioreactors: Break-up in turbulent flows," *The Chemical Engineering Journal*, vol. 32, no. 1, pp. B7-B17, 1986/02/01/ 1986.
- [81] J. Hinze, "Fundamentals of the hydrodynamic mechanism of splitting in dispersion processes," *AIChE Journal*, vol. 1, no. 3, pp. 289-295, 1955.
- [82] K. Sriram and R. Mann, "Dynamic gas disengagement: A new technique for assessing the behaviour of bubble columns," *Chemical Engineering Science*, vol. 32, no. 6, pp. 571-580, 1977.
- [83] W. K. Lewis and W. G. Whitman, "Principles of Gas Absorption," *Industrial & Engineering Chemistry*, vol. 16, no. 12, pp. 1215-1220, 1924/12/01 1924.
- [84] F. Yoshida and K. Akita, "Performance of gas bubble columns: Volumetric liquid-phase mass transfer coefficient and gas holdup," *AIChE Journal*, vol. 11, no. 1, pp. 9-13, 1965.
- [85] K. Akita and F. Yoshida, "Gas Holdup and Volumetric Mass Transfer Coefficient in Bubble Columns. Effects of Liquid Properties," *Industrial & Engineering Chemistry Process Design and Development*, vol. 12, no. 1, pp. 76-80, 1973/01/01 1973.
- [86] H. Hikita, S. Asai, K. Tanigawa, K. Segawa, and M. Kitao, "The volumetric liquid-phase mass transfer coefficient in bubble columns," *The Chemical Engineering Journal*, vol. 22, no. 1, pp. 61-69, 1981/12/01/ 1981.
- [87] Y. Kawase, B. Halard, and M. Moo-Young, "Theoretical prediction of volumetric mass transfer coefficients in bubble columns for Newtonian and non-Newtonian fluids," *chemical Engineering science*, vol. 42, no. 7, pp. 1609-1617, 1987.
- [88] A. Schumpe, A. Saxena, and L. Fang, "Gas/liquid mass transfer in a slurry bubble column," *Chemical Engineering Science*, vol. 42, no. 7, pp. 1787-1796, 1987.
- [89] A. Schumpe, W. D. Deckwer, and K. D. Nigam, "Gas-liquid mass transfer in three-phase fluidized beds with viscous pseudoplastic liquids," *The Canadian Journal of Chemical Engineering*, vol. 67, no. 5, pp. 873-877, 1989.
- [90] M. Johnson, G. Andre, C. Chavarie, and J. Archambault, "Oxygen transfer rates in a mammalian cell culture bioreactor equipped with a cell-lift impeller," (in eng), *Biotechnol Bioeng*, vol. 35, no. 1, pp. 43-9, Jan 5, 1990.

- [91] J. O. Kim and S. D. Kim, "Gas-Liquid mass transfer in a three-phase fluidized bed with floating bubble breakers," *The Canadian Journal of Chemical Engineering*, vol. 68, no. 3, pp. 368-375, 1990.
- [92] P. M. Wilkinson, H. Haringa, and L. L. Van Dierendonck, "Mass transfer and bubble size in a bubble column under pressure," *Chemical Engineering Science*, vol. 49, no. 9, pp. 1417-1427, 1994/05/01/ 1994.
- [93] L. A. Tribe, C. L. Briens, and A. Margaritis, "Determination of the volumetric mass transfer coefficient (kLa) using the dynamic "gas out–gas in" method: Analysis of errors caused by dissolved oxygen probes," *Biotechnology and Bioengineering*, vol. 46, no. 4, pp. 388-392, 1995.
- [94] S. Maalej, B. Benadda, and M. Otterbein, "Interfacial area and volumetric mass transfer coefficient in a bubble reactor at elevated pressures," *Chemical Engineering Science*, vol. 58, no. 11, pp. 2365-2376, 6// 2003.
- [95] R. Lau, W. Peng, L. G. Velazquez-Vargas, G. Q. Yang, and L. S. Fan, "Gas–Liquid Mass Transfer in High-Pressure Bubble Columns," *Industrial & Engineering Chemistry Research*, vol. 43, no. 5, pp. 1302-1311, 2004/03/01 2004.
- [96] K. Muroyama, K. Imai, Y. Oka, and J. i. Hayashi, "Mass transfer properties in a bubble column associated with micro-bubble dispersions," *Chemical Engineering Science*, vol. 100, pp. 464-473, 2013.
- [97] O. N. Manjrekar, "Hydrodynamics and Mass Transfer in Bubble Columns," 10076403 Ph.D., Washington University in St. Louis, Ann Arbor, 2016.
- [98] M. Bouaifi, G. Hebrard, D. Bastoul, and M. Roustan, "A comparative study of gas hold-up, bubble size, interfacial area and mass transfer coefficients in stirred gas–liquid reactors and bubble columns," *Chemical Engineering and Processing: Process Intensification*, vol. 40, no. 2, pp. 97-111, 2001/02/01/ 2001.
- [99] Y. Kawase, "The energy dissipation rate concept for turbulent heat and mass transfer in drag-reducing fluids," *International Communications in Heat and Mass Transfer*, vol. 17, no. 2, pp. 155-166, 1990/03/01/ 1990.

- [100] S. Godbole, A. Schumpe, Y. Shah, and N. Carr, "Hydrodynamics and mass transfer in non-Newtonian solutions in a bubble column," *AIChE journal*, vol. 30, no. 2, pp. 213-220, 1984.
- [101] F. Neme, L. Coppola, and U. Böhm, "Gas holdup and mass transfer in solid suspended bubble columns in presence of structured packings," *Chemical Engineering & Technology: Industrial Chemistry-Plant Equipment-Process Engineering-Biotechnology*, vol. 20, no. 5, pp. 297-303, 1997.
- [102] T. Tomida, F. Yusa, and T. Okazaki, "Effective interfacial area and liquid—side mass transfer coefficient in the upward two-phase flow of gas—liquid mixtures," *The Chemical Engineering Journal*, vol. 16, no. 2, pp. 81-88, 1978/01/01/ 1978.
- [103] A. Behkish, Z. Men, J. R. Inga, and B. I. Morsi, "Mass transfer characteristics in a large-scale slurry bubble column reactor with organic liquid mixtures," *Chemical Engineering Science*, vol. 57, no. 16, pp. 3307-3324, 2002/08/01/ 2002.
- [104] J. H. Kim, C. W. Jung, and Y. T. Kang, "Mass transfer enhancement during CO₂ absorption process in methanol/Al₂O₃ nanofluids," *International Journal of Heat and Mass Transfer*, vol. 76, no. Supplement C, pp. 484-491, 2014/09/01/ 2014.
- [105] R. D. Pomeroy, W. N. Lacey, N. F. Scudder, and F. P. Stapp, "Rate of Solution of Methane in Quiescent Liquid Hydrocarbons," *Industrial & Engineering Chemistry*, vol. 25, no. 9, pp. 1014-1019, 1933/09/01 1933.
- [106] S. R. Etminan, B. B. Maini, Z. Chen, and H. Hassanzadeh, "Constant-Pressure Technique for Gas Diffusivity and Solubility Measurements in Heavy Oil and Bitumen," *Energy & Fuels*, vol. 24, no. 1, pp. 533-549, 2010/01/21 2010.
- [107] R. El-Haj, A. Lohi, and S. R. Upreti, "Experimental determination of butane dispersion in vapor extraction of heavy oil and bitumen," *Journal of Petroleum Science and Engineering*, vol. 67, no. 1, pp. 41-47, 2009/07/01/ 2009.
- [108] M. Jamialahmadi, M. Emadi, and H. Müller-Steinhagen, "Diffusion coefficients of methane in liquid hydrocarbons at high pressure and temperature," *Journal of Petroleum Science and Engineering*, vol. 53, no. 1, pp. 47-60, 2006/08/01/ 2006.

- [109] Y. P. Zhang, C. L. Hyndman, and B. B. Maini, "Measurement of gas diffusivity in heavy oils," *Journal of Petroleum Science and Engineering*, vol. 25, no. 1, pp. 37-47, 2000/01/01/ 2000.
- [110] S. R. Upreti and A. K. Mehrotra, "Experimental Measurement of Gas Diffusivity in Bitumen: Results for Carbon Dioxide," *Industrial & Engineering Chemistry Research*, vol. 39, no. 4, pp. 1080-1087, 2000/04/01 2000.
- [111] M. R. Riazi, "A new method for experimental measurement of diffusion coefficients in reservoir fluids," *Journal of Petroleum Science and Engineering*, vol. 14, no. 3, pp. 235-250, 1996/05/01/ 1996.
- [112] H. M. Letzel, J. C. Schouten, R. Krishna, and C. M. van den Bleek, "Gas holdup and mass transfer in bubble column reactors operated at elevated pressure," *Chemical Engineering Science*, vol. 54, no. 13, pp. 2237-2246, 1999/07/01/ 1999.
- [113] R. F. Weiss, "The solubility of nitrogen, oxygen, and argon in water and seawater," *Deep Sea Research and Oceanographic Abstracts*, vol. 17, no. 4, pp. 721-735, 1970/08/01/ 1970.
- [114] O. N. Manjrekar and M. P. Dudukovic, "Application of a 4-point optical probe to a Slurry Bubble Column Reactor," *Chemical Engineering Science*, vol. 131, pp. 313-322, 2015/07/28/ 2015.
- [115] M. Shah, A. A. Kiss, E. Zondervan, J. van der Schaaf, and A. B. de Haan, "Gas Holdup, Axial Dispersion, and Mass Transfer Studies in Bubble Columns," *Industrial & Engineering Chemistry Research*, vol. 51, no. 43, pp. 14268-14278, 2012/10/31 2012.
- [116] A. Esmaeili, C. Guy, and J. Chaouki, "Local hydrodynamic parameters of bubble column reactors operating with non-Newtonian liquids: Experiments and models development," *AIChE Journal*, 2015.
- [117] B. C. Pak and Y. I. Cho, "HYDRODYNAMIC AND HEAT TRANSFER STUDY OF DISPERSED FLUIDS WITH SUBMICRON METALLIC OXIDE PARTICLES," *Experimental Heat Transfer*, vol. 11, no. 2, pp. 151-170, 1998/04/01 1998.
- [118] H. Jin, D. Liu, S. Yang, G. He, Z. Guo, and Z. Tong, "Experimental Study of Oxygen Mass Transfer Coefficient in Bubble Column with High Temperature and High Pressure," *Chemical Engineering & Technology*, vol. 27, no. 12, pp. 1267-1272, 2004.

- [119] H. Jin, S. Yang, G. He, D. Liu, Z. Tong, and J. Zhu, "Gas–Liquid Mass Transfer Characteristics in a Gas–Liquid–Solid Bubble Column under Elevated Pressure and Temperature," *Chinese Journal of Chemical Engineering*, vol. 22, no. 9, pp. 955-961, 2014/09/01/ 2014.
- [120] I. Dewes and A. Schumpe, "Gas density effect on mass transfer in the slurry bubble column," *Chemical Engineering Science*, vol. 52, no. 21, pp. 4105-4109, 1997/11/01/ 1997.
- [121] M. Fukuma, K. Muroyama, and A. Yasunishi, "SPECIFIC GAS-LIQUID INTERFACIAL AREA AND LIQUID-PHASE MASS TRANSFER COEFFICIENT IN A SLURRY BUBBLE COLUMN," *Journal of Chemical Engineering of Japan*, vol. 20, no. 3, pp. 321-324, 1987.
- [122] U. Jordan and A. Schumpe, "The gas density effect on mass transfer in bubble columns with organic liquids," *Chemical Engineering Science*, vol. 56, no. 21, pp. 6267-6272, 2001/11/01/ 2001.